Outcrop and core integrative ichnofabric analysis of Miocene sediments from Lepe, Huelva (SW Spain): improving depositional and paleoenvironmental interpretations

Francisco J. Rodríguez-Tovar [a,*], Javier Dorador [a], Eduardo Mayoral [b], Ana Santos [a]

[a] *Departamento de Estratigrafía y Paleontología, Universidad de Granada, 18071-Granada (Spain)*

[b] *Departamento Ciencias de la Tierra, Universidad de Huelva, 21071, Huelva (Spain)*

* Corresponding author: fjrtovar@ugr.es (F.J. Rodríguez-Tovar)

ABSTRACT

Ichnofabric analysis was conducted in Miocene sediments from Lepe (Huelva, SW Spain) based on integrative outcrop and core research, to improve interpretations of depositional and paleoenvironmental conditions, with special attention to sequence stratigraphy. Seven intervals were differentiated in outcrops based on stratigraphic and ichnological features, consisting of two ichnofabrics: *Ophiomorpha-Thalassinoides-Spongeliomorpha* ichnofabric characterizes intervals 1, 2, 6, 7 and 8, while *Palaeophycus-Planolites-Phycosiphon* ichnofabric characterizes intervals 3, 4 and 5. Fourteen ichnofabrics were differentiated in core, mainly in view of lithological features, including ferruginous material, grain size, mottled background, ichnotaxa, and Bioturbation Index. A comparison between outcrop and core ichnofabrics through the upper 13.5 m, corresponding to the uppermost Tortonian-lowermost Messinian interval, revealed certain similarities as well as some differences. A continuous siliciclastic deposition with punctual variations in the sedimentation rate can be interpreted that, associated with favorable paleoenvironmental parameters such as aerobic conditions and nutrient availability, allow the maintenance of a well-developed and diverse macroinvertebrate trace maker community. Softgrounds are dominant, but punctually loosegrounds and even firmgrounds could develop. The ichnofabric distribution shows long-scale patterns in outcrop and core, and short-scale patterns exclusively in core. Long-scale patterns reflect the last phases of a transgressive system tract, with a "maximum flooding zone" at the end, and then a highstand normal regression. High-frequency, short-scale, repetitive patterns in ichnofabrics from core, mainly between ichnofabrics 6 and 8 (below) and 9 (above), can be linked to "local flooding surfaces", subdividing the "maximum flooding zone" into parasequences.

Keywords: Ichnofabrics, outcrop and core, paleoenvironmental conditions, sequence stratigraphy, maximum flooding zone, local flooding surfaces, Miocene, Huelva

1. Introduction

During recent years ichnological analysis has become a useful innovative tool for basin analysis and paleoenvironmental studies, evidencing relationships between trace makers´ behavior and the prevailing paleoenvironmental conditions (i.e., Buatois and Mángano, 2011; Knaust and Bromley, 2012). The ichnofabric approach, as a branch of trace fossil analysis, is based on the integration of information about various aspects of the texture and internal structure of a substrate resulting from bioturbation and bioerosion at any scale —e.g. primary sedimentary structures, ichnological diversity, amount of bioturbation, cross-cutting relationships and tiering— can be applied to many disciplines in Earth Sciences. This approach holds a high potential in the characterization of sedimentary environment and paleoenvironmental reconstructions, lending greater precision to high-resolution studies (i.e., Buatois and Mángano, 2011; Ekdale et al., 2012). However, because it stands as a relatively new method in ichnological research, its usefulness in basin analysis has been scarcely tested to date.

The case at hand involves Miocene sediments from Lepe (Huelva, SW Spain). From the second half of the nineties profuse paleoichnological research has been conducted in Miocene sediments from Lepe and surrounding areas. A complete characterization of the trace fossil assemblage based on a detailed ichnotaxonomical differentiation has led to general paleoenvironmental reconstructions of the depositional area during this period (i.e., Mayoral and Muñiz, 1995, 1996, 1998, 2001; Muñiz et al., 1998, 2010, 2015; Muñiz and Mayoral, 1999, 2001a, b; Belaústegui et al., 2016). The aforementioned ichnological research, based exclusively on outcrops, allows for the recognition of tri-dimensional structures and ichnotaxonomy, but in

cases entails limitations due to scarce vertical continuity, significant weathering, or preservation.

In this paper we present an integrative ichnological research effort, studying the Miocene sediments in Lepe through the ichnofabric analysis of outcrops and cores, to improve interpretation of the sedimentary environment, including temporal variations in paleoenvironmental conditions.

2. Geological setting. The studied section

The studied area is located on the outskirts of the town of Lepe (Huelva province, SW Spain), which geologically corresponds to the western sector of the Guadalquivir Basin (Fig. 1). It is a foreland basin developed during the Neogene and Quaternary, between the External Zone of the Betic Cordillera, its southern limit, and the Paleozoic basement of the Iberian Massif, its passive northern margin (Sierro et al., 1996). The Guadalquivir Basin has an ENE-WSW elongated triangular shape with remarkable asymmetry; it formerly opened to the Mediterranean Sea and to the Atlantic Ocean (Tortonian – Early Messinian), but currently only towards the Atlantic (Gulf of Cadiz) (Fig. 1).

Core and outcrop analyses were conducted on Upper Miocene sediments, close to the so-called “Catalán road” between Valsequillo creek and Cabezo del Silbado (Fig. 1).

To date, research on the Miocene in this sector has focused on the area of Cabezo de La Zarcilla, located about 1 km to the NNW (Mayoral and Muñiz, 1994, 1995, 2001; Muñiz, 1998; Muñiz and Mayoral, 1999, 2001a; Muñiz, et al., 1998, 2010; Belaústegi et al., 2016). Cabezo de La Zarcilla area (Muñiz, 1998) comprises three sections, named LE9 (from Lepe to 1.5 km to the South, along the road to Antilla village), LE10 (Cabezo del Silbado) and LE11 (from the point named "First Cross" to Cabezo de La Zarcilla). This clarification is important because the list of trace fossils mentioned in Muñiz et al. (2010) and Belaústegi et al. (2016) corresponds to the sum

of those found in the three sections (LE9, LE10 and LE11), not exclusively to the Cabezo de la Zarcilla section (LE 11).

Five lithological units recognized in this area (Muñiz et al., 2010; Belaústegi et al., 2016) consist of a coarsening upward sequence from blue mudstones (unit 1) to white sandy silts (unit 2) and to sandy facies (units 3, 4, and 5). These last three units include fine-grained sands with glaucony (unit 3), medium- to coarse-grained sands with carbonate concretions (unit 4) and medium- to coarse-grained sands with abundant preserved invertebrate shells (unit 5). Radiometric dating of the glaucony in unit 3 (Mayoral and Muñiz, 1994) yielded ages of -6.6±0.3 and -6.7±0.3 Ma, which correspond to the Messinian (Late Miocene). Bivalves and gastropods in unit 4 apparently indicate a similar age, while calcareous nannoplankton from the same unit corresponds to biozone CN9, which is Upper Tortonian-Messinian (Muñiz et al., 2001b). Muñiz et al. (2010) remark that dating of unit 5 is problematic since calcareous nannoplankton corresponds to biozone CN11 (Late Zanclean) (Muñiz et al., 2001b), while the malacofauna indicate an Upper Miocene age.

This disparity is reflected in Belaústegi et al. (2016), where the authors give unit 5 two different ages at the same time, Upper Miocene and Lower Pliocene, arguing the existence of an erosional surface (a supposedly intra-sandy level). However, this erosional truncation is reflected in the stratigraphic log (figure 1C, pag. 81) between units 5 and 6, which is clearly Pliocene. Abad et al. (2013), studying La Antilla section, around 2 km south, found a hummocky cross-stratification at the boundary between the Miocene and Pliocene, related with large storm waves possibly from hurricanes. These authors evoke an erosional surface atop unit 5 (the malacofauna-rich sandy level), yet this unit is not observed in La Antilla section. Thus they hypothesize the existence of a significant reworking process of the Miocene units during the Pliocene, which would cover a significant stratigraphic hiatus including at least part of the Messinian and

Zanclean (lower Pliocene).

The present study was carried out on unit 2, a siliciclastic facies informally known as 'Lepe White Silts' (Muñiz et al., 2010; Belaústegi et al., 2016) that unconformably lies upon Lower Carboniferous greywackes and shales, Upper Miocene in age (Upper Tortonian-Messinian; Muñiz et al., 2001a; Muñiz et al. 2010).

2.1. Stratigraphy

Detailed outcrop analysis involved examining 13.5 m of unit 2, constituted by the following intervals (Fig. 2):

Interval 1: Corresponds to 1.4 m-thick gray sandy silts, greenish inside, with a ferruginous horizon at the top. *Ophiomorpha* isp. and *Phycosiphon* isp. are present in the upper part of the interval, with large *Thalassinoides suevicus* at the bottom.

Interval 2: Consists of 1.3 m-thick white sandy silts with diffuse mottled background and a ferruginous crust at the top. It contains *Ophiomorpha nodosa, Phycodes palmatus, Rosselia* isp., and *Spongeliomorpha sinuostriata*. Near the top appear *Palaeophycus striatus, Skolithos* isp., *Teichichnus* isp., and *Thalassinoides* isp.

Interval 3: Characterized by 1.2 m-thick white fine grained silts, with thin and discontinuous ferruginous levels inside, showing mottled appearance. The uppermost part of this interval shows *Phycodes ungulatus*, *Phycosiphon* isp., *Skolithos* isp., *Spongeliomorpha chevronensis, Taenidium* isp., *Teichichnus* isp., and *Thalassinoides suevicus*. The middle part of the interval contains *Planolites* isp., *Spongeliomorpha sinuostriata* and *Thalassinoides* isp., as well as bioerosion structures, such as *Gastrochaenolites* isp., which appear on ferruginous internal molds of *Thalassinoides* isp. Horizontal lamination is locally observed.

Interval 4: Consists of 1.3 m-thick white sandy silts, sparsely mottled, with well-defined

ferruginous horizons inside and with a prominent crust on top. Low angle cross-lamination is observed in the upper half of the interval. *Ophiomorpha* isp., and *Thalassinoides* isp., are found all across the interval, while *Cheiichnus* isp., *Ophiomorpha nodosa, Palaeophycus* isp., *Phycodes palmatus*, *Planolites* isp., *Rosselia* isp., and *Teichichnus rectus* are located just below the ferruginous crust. This crust shows locally isolated *Gastrochaenolites* isp.

Interval 5: Corresponds to 1 m-thick white fine grained silts with a well-defined mottled background and horizontal lamination, containing *Phycosiphon* isp., and *Planolites* isp.

Interval 6: Shows 2.1 m-thick white fine sands, gray-greenish inside, with a well-developed ferruginous crust on top. Ferruginous material is locally present, with a mottled appearance. This interval contains *Diplocraterion paralellum*, *Ophiomorpha* isp., *Planolites* isp., *Spongeliomorpha chevronensis, S. sinuostriata*, *Thalassinoides* isp., and *T. suevicus*. On the crust, only *Palaeophycus* isp. is present. Horizontal lamination is observed in the lower half of the interval.

Interval 7: Consists of 4.2 m-thick white to pinkish-grayish sandy silts with ferruginous crusts in the upper meter of the interval. The lower-half part is characterized by the presence of *Ophiomorpha* isp., *O. nodosa*, *Thalassinoides* isp., and *T. suevicus*. The uppermost part, associated with the ferruginous levels, shows *Cheiichnus* isp., *Conichnus* isp., *O. nodosa*, *Palaeophycus tubularis*, *Spongeliomorpha sinuostriata, Taenidium* isp., and *Thalassinoides* isp. Some disperse ferruginous internal molds of venerid and pectinid bivalves are found in the lower and upper parts of the interval, respectively. Local cross-lamination is observed.

Interval 8: Characterized by 1.5 m-thick fine to medium gray sands with *Gyrolithes variabilis, Spongeliomorpha chevronensis, S. sinuostriata*, and *Thalassinoides* isp.

According to Muñiz et al. (2010), unit 2 of La Zarcilla section (which corresponds to La

Zarcilla area, as stated above), presents common mollusks, mostly bivalves, but also gastropods and scaphods, and some decapods (cheliped fragments of callianassid shrimps). Other fossils, such as cephalopods (cuttlefish), solitary corals, fish teeth and cetacean bones, are rarer, but also present. From all these fossils, only bivalves have been found in interval 7 of the studied log.

3. Methods

The applied methodology should be differentiated according to the study of outcrops and cores. Ichnological research in outcrops has developed following standard procedures in the field and drawing the graphic lithological log. Care was taken to register occurrences of trace fossils to establish the ichnofabric characteristics, such as trace fossil assemblage, tiering, cross-cutting relationships and bioturbation index, among others. Trace fossils samples were collected when it was deemed appropriate for detailed study in the laboratory. Photographs of general views and close-ups were obtained to complete the description of the outcrops.

The studied cores were drilled using a Rolatec RL 48 L (Fig. 3). Cores were obtained by means of two techniques —percussion (collecting 76 mm diameter cores) and rotation (101 mm diameter cores)— depending on the resistance of the drilled layer. These techniques were applied without perforating the fluid system to avoid the missing of sandy material due to the features of the studied materials. The studied core (Lepe S1) was drilled from 0 to 37.6 m depth, obtaining a long continuous record mainly composed by sandy materials. The ichnofabric characterization took into account lithology, color, degree of bioturbation, trace fossil assemblage, existence of mottled background, and presence of iron oxide and sedimentary structures. Lithology and grain size were determined using the grade scale proposed by Wentworth (1922) and Shepard's classification scheme (Shepard, 1954), and color was defined using the Munsell color system. The degree of bioturbation was determined according to the Bioturbation Index (Taylor and

Goldring, 1993), based on a scale from BI=0 (unbioturbated) to BI=6 (completely bioturbated). Although the index was determined considering discrete trace fossils, they were often identified over a mottled background. The presence of iron oxide, sedimentary structures or other particular features was also considered. This detailed ichnofabric analysis was conducted in the entire core (37.6 m-thick; see Figs. 8-11), but comparison with outcrop data only refers to the upper 13.5 m (Figs. 4, 12).

The simultaneous analysis of ichnofabrics in outcrops and cores helps one discern the advantages and disadvantages of each method. In general, the field analysis facilitates a three-dimensional view of fossils and trace fossils and their lateral extension. This spatial perception is crucial for identifying trace fossils that appear on the ferruginous crusts, which have substantial development in the study area. However, analysis of the core samples provides for greater precision in identifying small trace fossils, especially those that have not been ferruginized. The cores moreover lend greater control of the grain size and its vertical variations along the stratigraphic series.

4. Results. Paleoichnological and sedimentological analysis

4.1. Trace fossil assemblages and ichnofabrics in outcrop

Muñiz et al. (2010) and Belaústegi et al. (2016) mention the existence of 27 ichnotaxa in the studied unit (in La Zarcilla section, corresponding to La Zarcilla area), composed by *Arenicolites*, *Bergaueria*, *Bichordites*, *Cardioichnus*, *Conichnus*, *Cheiichnus*, *Gyrolithes*, *Haentzschelinia*, *Helicolithus*, *Helminthopsis*, *Lepeichnus*, *Lockeia*, *Macanopsis*, cf. *Monomorphichnus*, *Nereites*, *Ophiomorpha*, *Palaeophycus*, *Phycodes*, *Psilonichnus*,

Rusophycus, *Scolicia*, *Skolithos*, *Spongeliomorpha*, *Taenidium*, *Teichichnus*, *Thalassinoides*, and cf. *Torrowangea*. These authors also indicated the existence of three different trace fossil assemblages for this unit according to previous studies of Muñiz (1998) and Muñiz et al. (1998). In our opinion, these ichnoassemblages can be considered ichnoassociations (Gámez Vintaned and Mayoral Alfaro, 1992), "the ichnotaxon or ichnotaxa which are recurrently present in a number of ichnocoenoses", rather than an ichnoassemblage, a basic, descriptive concept that refers to a set of trace fossils found in a bed or beds of a given locality. Accordingly, and following the original description of Muñiz (1998) and Muñiz et al. (1998): a) the lower part of the studied unit was characterized by an *Ophiomorpha-Skolithos* ichnoassociation, dominated by these two ichnogenera along with *Thalassinoides*; b) the middle part is represented by the *Gyrolithes variabilis* ichnoassociation, accompanied by most of the ichnogenera mentioned above; and c) the upper part consists of less common *G. variabilis*, the *Spongeliomorpha–Teichichnus–Phycodes* ichnoassociation being dominant, with these three ichnotaxa commonly forming compound structures.

In the Cabezo del Silbado section the sediments vary from silts to fine grained sands and color is from white, greenish inside, to gray-pinkish. The Bioturbation Index ranges from 0 to 3. The trace fossil assemblage is made up of 16 ichnotaxa: *Cheiichnus*, *Conichnus*, *Diplocraterion*, *Gastrochaenolites*, *Gyrolithes*, *Ophiomorpha*, *Palaeophycus*, *Phycodes*, *Phycosiphon*, *Planolites*, *Rosselia*, *Skolithos*, *Spongeliomorpha*, *Taenidium*, *Teichichnus*, and *Thalassinoides*. Iron oxide is characteristic of these sediments, permeating most trace fossils, and the presence of ferruginous crusts, with a remarkable development and extension, is frequent. Horizontal lamination or low angle cross-lamination is locally present. Glaucony grains were not found.

According to these features, the following ichnofabrics in outcrops were identified (Fig. 4):

***Ophiomorpha-Thalassinoides-Spongeliomorpha* ichnofabric.** It characterizes intervals 1, 2, 6, 7 and 8 (Figs. 4, 5A, 6). White to gray, pinkish, greenish-grayish inside, sandy silts to fine sands. Not or sparsely mottled. Trace fossil diversity is moderate to high, composed by dominant *Ophiomorpha* isp., *O. nodosa* (Fig. 7P), *Thalassinoides* isp. (Fig. 7L), *T. suevicus*, *Spongeliomorpha chevronensis*, and *S. sinuostriata* (Fig. 7K). Subordinate ichnotaxa are *Cheiichnus* isp. (Fig. 7I), *Conichnus* isp. (Fig. 7J), *Diplocraterion paralellum*, *Gyrolithes variabilis* (Fig. 7O), *Palaeophycus* isp., *P. striatus*, *P. tubularis* (Fig. 7M), *Phycode*s isp., *P. palmatus*, *Phycosiphon isp.*, *Planolites* isp. (Fig. 7L), *Rosselia* isp., *Skolito*s isp., *Taenidium* isp., and *Teichichnus* isp. Ferrugenized horizons are locally present. Moreover, most of the traces are also ferrugenized. Bioturbation Index is low (0-2), and occasionally moderate (3) at the top of interval 7.

Most trace fossils (about 70%) occupy the shallower horizons (tiers 1-3), tier 1 corresponding to iron surfaces, tier 2 to the first 15 cm deep, tier 3 from 15 to 50 cm deep and tier 4, more than 50 cm in depth (Fig. 5A). *Thalassinoides* isp., and *Ophiomorpha nodosa* are at lower levels of occupation, the corresponding trace makers being those with greater exploitation capacity and reworking of sediments. It is common for both to be overprinted by the next generation of burrowers, usually *Spongeliomorpha sinuostriata*, *S. chevronensis*, and *Thalassinoides suevicus* (Fig. 5A).

***Palaeophycus-Planolites-Phycosiphon* ichnofabric.** It characterizes intervals 3, 4 and 5 (Figs. 4, 5B, 6). White silts to sandy silts. Not mottled or slightly and locally mottled. Trace fossil diversity is slightly lower than in the previous one, and composed by *Palaeophycus* isp. (Fig. 7Q), *Phycosiphon* isp., and *Planolites* isp. *Thalassinoides* isp., *Teichichnus* isp., and *T.*

rectus (Fig. 7G-H) are also frequent. Subordinate ichnotaxa are: *Cheiichnus* isp., *Ophiomorpha* isp., *O. nodosa* (Fig. 7D), *Phycodes palmatus* (Fig. 7A), *P. ungulatus*, *Rosselia* isp. (Fig. 7B-C), *Skolithos* isp., *Spongeliomorpha chevronensis*, *S. sinuostriata*, *Taenidium* isp. (Fig. 7N), and *Thalassinoides suevicus*. Ferruginous material and crusts are frequent. The degree of bioturbation is low to moderate (BI: 0-3), with the maximum value just below the ferruginous crusts. Worth noting is the existence of bioerosional structures (*Gastrochaenolites* isp.) both on the ferruginous surface crusts and in *Thalassinoides* isp. (Figs. 7E-F).

As occurs in the previous case, shallower levels show a higher degree of occupation (Fig. 5B). *Thalassinoides*, *Ophiomorpha*, and *Spongeliomorpha* are also registered in deeper horizons, though rarely found below 50 cm depth.

4.2. Trace fossil assemblages and ichnofabrics in core Lepe S1

The trace fossil assemblage in the entire core Lepe S1 (37.6 m thick) consists of 10 ichnotaxa (at the ichnogenus level): *Conichnus*, *Gyrolithes*, *Macaronichnus*, *Ophiomorpha*, *Phycodes*, *Phycosiphon*, *Planolites*, *Schaubcylindrichnus*, *Teichichnus*, and *Thalassinoides* (Fig. 4). Overall, according to lithology and grain size, the sediments vary from silt to medium-coarse grained sands and color is comprised between different values within the yellow hues of the Munsell Code. Bioturbation is variable, from absent (no mottled background or discrete traces) to a well-defined mottled background, overprinted by relatively abundant discrete trace fossils. Bioturbation Index values for discrete trace fossils range from 0 to 3. Iron oxide presence varies from absent to abundant and cross lamination is locally identified. Additionally, in some cases other relevant features were considered, such as the presence of peloids, quartz grains or glaucony. All these features (Table 1), allow for the characterization of 14 ichnofabrics (sorted according to grain size; Figs. 8, 10):

Ichnofabric 1: No mottled siltstone. Light gray (2.5Y 7/1) silty sediments characterized by the absence of mottled background and the scarce presence of discrete trace fossils; *Phycosiphon* and *Planolites*, with the local presence of ferrugenized *Thalassinoides*. Bioturbation Index is low (0-1). High presence of drilling lamination induced structures. This ichnofabric is observed from 36.00-35.00 m and 29.00-27.55 m. Gradual lower and upper transition to the corresponding ichnofabrics below and above.

Ichnofabric 2: Mottled very fine to fine grained silty sandstone without discrete traces. Pale yellow (2.5Y 7/3) silty sand, very fine to fine grained, characterized by the presence of large-evident mottled background. Discrete traces are absent, except for the local record of *Planolites* (BI: 0-1). Variable presence of ferruginous material with a mottled appearance. It is observed at 37.45-37.20 m, 36.65-36.45 m, 34.00-33.40 m, 33.00-30.50 m, 30.00-29.00 m and 27.25-26.60 m; while it is the most abundant ichnofabric, there are differences according to the variable presence of ferruginous background. It reveals a gradual lower and upper transition mainly with ichnofabric 3, "*Mottled very fine to fine grained silty sandstone with discrete traces*".

Ichnofabric 3: Mottled very fine to fine grained silty sandstone with discrete traces. Pale yellow (2.5Y 7/3) silty sand, very fine to fine grained, characterized by the presence of a very evident mottled background. Discrete trace fossils are observed as *Gyrolithes*, *Planolites* and *Thalassinoides*. Bioturbation Index is low to moderate (BI: 2-3). Local peloids are observed and ferruginous background is dominant. This ichnofabric could be considered as transitional with the previous one in light of the increased ferruginous background and discrete traces. Induced drilling lamination is locally present. It is observed at 37.60-37.45 m, 37.20-36.65 m, 36.45-36.00 m, 35.00-34.00 m, 33.40-33.00 m and 30.50-30.00 m.

These three ichnofabrics (1, 2 and 3) are dominant and exclusively present in the lowest

296 part of the core.

297 **Ichnofabric 4: Scarcely mottled very fine to fine grained silty sandstone with**
298 **discrete trace fossils.** White (2.5Y 8/1) silty, very fine to fine grained sand. This ichnofabric
299 shows a diffuse mottled background overprinted by discrete traces as *Planolites*, and
300 *Thalassinoides*. The degree of bioturbation is low to moderate (BI: 2-3). Locally, well-defined
301 ferruginous material is identified. This ichnofabric is present at 24.60-24.00 m, 23.20-22.60 m
302 and 21.00-20.65 m.

303 **Ichnofabric 5: Non-mottled very fine to fine grained silty sandstone with scarce**
304 **trace fossils.** White (2.5Y 8/1) silty, very fine to fine grained sand. Mottling is absent and
305 discrete trace fossils, as *Phycodes*, are scarce. Bioturbation Index is low (0-1) and there is no
306 presence of ferruginous material. It is found at 19.65-18.45 m and 2.00-1.00 m.

307 **Ichnofabric 6: Sparsely mottled very fine to fine grained silty sandstone with**
308 **discrete trace fossils.** White (2.5Y 8/1) silty, very fine to fine grained sand, with a sparsely
309 mottled background overprinted by discrete trace fossils including *Palaeophycus*, *Planolites*,
310 *Phycosiphon*, and *Schaubcylindrichnus*. Bioturbation Index is low (1-2) and ferruginous material
311 is locally present. It is found at 18.45-17.90 m, 16.70-16.45 m, 15.65-15.05 m, 14.90-14.70 m,
312 14.50-13.90 m, 12.00-11.00 m, 8.50-7.50 m, 6.60-6.00 m and 2.45-2.00 m. This ichnofabric is
313 the most abundant and widely distributed ichnofabric in the upper half of the studied section.

314 **Ichnofabric 7: Great mottled fine grained sandstone with ferruginous discrete**
315 **traces.** Pale yellow (2.5Y 8/2) fine grained sand with large and well-defined mottled background
316 overprinted by discrete trace fossils. These ichnotaxa are commonly highly ferruginized, as
317 *Gyrolithes*, and *Thalassinoides*, or non-ferrugenized as *Planolites*. Low to moderate Bioturbation
318 Index between 2 and 3; ferruginous material is abundant, mostly infilling traces, and thus having
319 a conspicuous appearance. It is characterized at 27.55-27.25 m, 26.60-26.00 m, 25.30-24.65 m

and 21.40-21.00 m.

Ichnofabric 8: Non-mottled fine grained sandstone with discrete trace fossils. Pale yellow (2.5Y 8/3) fine grained sand, without mottling and a sparse presence of discrete traces as *Planolites* or ferrugenized *Ophiomorpha* and *Teichichnus*. The degree of bioturbation is low (BI: 1) and ferruginous material presence is diffuse. It is located at 10.40-10.00 m and 9.60-8.70 m.

Ichnofabric 9: Non-mottled fine to medium grained sandstone with ferruginous discrete traces. Pale yellow (2.5Y 8/2) fine to medium grained sand sediment with ferruginous discrete traces as *Ophiomorpha*, *Planolites*, *Schaubcylindrichnus*, and *Teichchnus*; *Ophiomorpha* and *Teichichnus* are well developed and highly ferruginized. Mottled background is absent and the Bioturbation Index is low to moderate (BI: 2-3). Probable local presence of cross lamination. This ichnofabric is located at 20.60-20.00 m, 19.90-19.70 m, 17.00-16.70 m, 15.85-15.65 m, ¿12.25-12.00 m?, 11.00-10.70 m, 10.00-9.65 m, 8.70-8.55 m, 7.50-6.80 m and 1.00-0.80 m. It is characterized by the best examples of large ferruginous traces with good specimens of *Ophiomorpha* and *Teichichnus*.

Ichnofabric 10: Non-mottled fine to medium grained sandstone with quartz grains and discrete traces. Light gray (2.5Y 7/2) fine to medium grained sand without mottling. It is characterized by the presence of quartz grains and the absence of ferruginous material. Discrete traces are clearly observed as *Macaronichnus* (only registered in this ichnofabric), *Ophiomorpha*, and *Planolites*. Bioturbation Index is low to moderate (2-3). This ichnofabric is only locally observed, between 10.70 and 10.40 m.

Ichnofabric 11: Non-mottled fine to medium grained sandstone with punctual discrete traces. Light gaey (2.5Y 7/2) fine to medium grained sand without mottled background. Punctual discrete traces are identified, sometimes with ferruginous infilling. *Ophiomorpha*, *Planolites*, and *Thalassinoides* are identified and Bioturbation Index varies from 1 to 2. It is

located at 6.75-6.60 m, 6.00-4.90 m and 4.70-2.45 m. Locally, cross lamination is well developed (from 4.00 to 3.70) and peloids are observed.

Ichnofabric 12: Non-mottled medium grained sandstone with glaucony. White (5Y 8/1) medium grained sand sediment, characterized by no mottled background and a clear presence of glaucony grains. Discrete traces are scarce, as *Gyrolithes*, with a low bioturbation degree (BI: 1.-2). No ferruginous material is observed. It is located at 25.95-25.40 m and 22.40-22.00 m.

Ichnofabric 13: Non-mottled medium grained sandstone with cross lamination and peloids. White (5Y 8/1) medium grained sand without mottling and presence of scarce discrete traces of *Gyrolithes*, *Planolites*, and *Thalassinoides*. Bioturbation Index is between 1 and 2. Cross lamination is relatively well-developed and peloids are abundant. Ferruginous material is nearly absent. This ichnofabric is located at 24.00-23.20 m, 22.55-22.40 m and 22.00-21.40 m.

Ichnofabric 14: Unconsolidated medium to coarse grained sandstone with Q grains and without mottling. Pale yellow (2.5Y 7/3) medium to coarse grained sandstone with scarce trace fossils of isolated *Phycodes* and *Conichnus* (BI: 0-1). It is located at 20.00-19.90 m, 17.85-17.15 m, 16.40-15.85 m, 15.00-14.90 m, 14.65-14.50 m, 13.90-12.35 m and 4.90-4.75 m. Lamination can be envisaged.

Additionally, some iron crustal thin horizons, without bioturbation, were identified across the core (Fig. 8).

Regarding the record of these ichnofabrics, several interesting features deserve mention. Some of the ichnofabrics are identified once or twice across the core, for instance ichnofabrics 1, 5 or 10, while ichnofabrics 6 and 9 are identified eight and nine times, respectively. However, the latter are recognized continuously in a maximum range of 1 m, a shorter record than ichnofabrics 1, 5 or 11, which are mostly recognized in a more continuous interval longer than 1

m. Another interesting feature is the relative abundance of ichnofabrics throughout the entire core (Fig. 9). The ones identified in very fine-fine grained sandstones (ichnofabrics 2 to 6) represent over 45% of the core, and those identified in fine-medium grained sandstones more than 25%. The most abundant ichnofabrics are 2 and 6, each representing almost 14% of the core. Then, there is a group of six ichnofabrics (1, 3, 5, 7, 9, 11 and 13) that oscillate between 5% and 10%; the rest are identified in less than 5% of the core in each case.

4.3. Ichnofabric distribution

Distribution of ichnofabrics reveals long- and short-scale patterns. Long-scale patterns are observed in both outcrop and core. However, a differentiation at the short scale is much more difficult to establish in outcrop —the inability to accurately characterize the transition between them makes it impossible to detail changes in patterns or trends. Thus, short-scale patterns have only been differentiated in core (Fig. 10).

4.3.1. Long-scale distribution

As pointed out above, just two ichnofabrics were distinguished in outcrop. *Ophiomorpha-Thalassinoides-Spongeliomorpha* ichnofabric characterizes the lower and upper parts of the section (intervals 1-2, between around 13.5 m and 11 m, and intervals 6 to 8, between roughly 7.5 and 0 m), whereas the *Palaeophycus-Planolites-Phycosiphon* ichnofabric is restricted to the middle part (intervals 3-5, between around 7.5 m and 11 m).

At core, a clear differentiation can be made between the lower and the upper parts of the entire section, with ichnofabrics exclusive to either part (Figs. 10, 11):

a) The lower part of the section (from the bottom to around 21 m; Figs. 10, 11), shows a

391 dominance, near exclusiveness, of fine to very fine ichnofabrics characterized by a mottled
392 background (mainly ichnofabrics 2 and 3, but also 4 and 7). The record of non-mottled
393 ichnofabrics is only punctually observed (ichnofabrics 1, 12 and 13). In this context, there is a
394 clear trend of increased grain size between the lower half of this lower part, characterized by
395 very fine to fine grained ichnofabrics (1, 2 and 3), and the upper half of this lower part, with
396 dominance of fine to medium grained ichnofabrics (7, 12 and 13).
397 b) The upper part of the section (from around 21 m to the top; Figs. 10, 11), reveals a
398 generalized increase of grain size, with a dominance of medium to coarse grained ichnofabrics
399 (ichnofabrics 9, 10, 11, and 14), and less abundant very fine to fine grained ones (ichnofabrics 5
400 and 6). This part is also characterized by a higher abundance of non-mottled ichnofabrics (5, 8, 9,
401 10, 11 and 14) with respect to mottled ones (ichnofabric 6). In this context, a clear differentiation
402 is observed between the lower half (between meter 18 and 12) of this upper part, characterized
403 by the presence of coarser ichnofabrics (ichnofabric 14) and the record of iron crusts (number 15
404 in Fig. 11), and the upper half of this upper part (from meter 12 to the top), with dominance of
405 non-mottled fine to medium grained ichnofabrics (ichnofabrics 9 and 11).
406
407 *4.3.2. Short-scale distribution*
408 The analysis of the two long-scale differentiated parts at the entire core reveals several
409 patterns/trends at the short-scale that can be characterized when the transitions between different
410 ichnofabrics are quantified (Dorador and Rodríguez-Tovar, 2016; Table 2):
411 a) In the lower part of the section (from the bottom to around meter 21), characterized by
412 mottled background ichnofabrics, a clear alternance/pattern is observed according to the absence
413 or presence of discrete trace fossils (italic values in Table 2). This general pattern is mainly

observed in the first meters of the core (from bottom to around meter 28), with the alternation between ichnofabric 2 (*mottled very fine to fine grained silty sandstone without discrete traces*), and ichnofabric 3 (*mottled very fine to fine grained silty sandstone with discrete traces*); 67.2% of transitions are from ichnofabric 2 to 3, and 83% from 3 to 2 (Table 2). This pattern is punctually interrupted by the presence of ichnofabrics 1 (*non-mottled siltstone*); there is a 50% of transitions from ichnofabrics 1 to 3 (Table 2). Above, from meter 28 to the top of the lower part of the section (around meter 21), an alternation is observed according to absence or presence of ferruginous discrete traces, between ichnofabrics 7 (*great mottled fine grained sandstone with ferruginous discrete traces*) and ichnofabrics 4 (*scarcely mottled very fine to fine grained silty sandstone with discrete trace fossils*), with a 50% of transitions between ichnofabrics 7 and 4. This pattern is punctually interrupted by the presence of non-mottled ichnofabrics 12 (*non-mottled medium grained sandstone with glaucony*) and 13 (*non-mottled medium grained sandstone with cross lamination and peloids*).

b) In the upper part of the section (from around meter 21 to the top), significant short-scale patterns are recognized in both the lower and the upper halves (non-italic values in Table 2). In the lower half, a repetitive pattern (around six times) is observed, with the presence of iron crusts in the base, and then decreasing grain size to the top, from *medium to coarse grained sandstone* (ichnofabric 14) above the iron crust, then *non-mottled fine to medium grained sandstone with ferruginous discrete traces* (ichnofabric 9), with 42.7% of transitions, and finally, on top, *sparsely mottled very fine to fine grained silty sandstone with discrete trace fossils* (ichnofabric 6), with 44.2% of transitions. Punctually, some of the ichnofabrics in this pattern might be absent. In general, a pattern can be envisaged in the upper half, characterized by the presence of ichnofabric 9 or ichnofabric 11 at the base, and then *sparsely mottled very fine to fine grained silty sandstone with discrete trace fossils* (ichnofabric 6), with 44.2% of transitions from

ichnofabric 9, and 66.6% from ichnofabric 11.

4.4. Outcrop vs core ichnofabrics

After characterizing ichnofabrics in the outcrop (around 13.5 m) and the entire core (around 37.5 m), a detailed comparison of the ichnofabric features was made for the correlated interval, corresponding to the upper 13.5 m of the core and the entire outcrop section (Figs. 4, 12).

Concerning the trace fossils assemblage (Fig. 4), certain similitudes and differences can be pointed out. Ichnotaxa such as *Ophiomorpha* isp., *Phycosiphon* isp., *Planolites* isp., *Skolithos* isp., *Teichichnus* isp., and *Thalassionides* isp., were similarly recorded in the ichnofabrics of the core and the corresponding intervals of the outcrop series. As for differences: a) Core analysis evidences the presence of discrete trace fossils that are hardly perceptible in the field, especially in traces not enhanced by ferruginization. Such is the case of *Macaronichnus* (ichnofabric 10, corresponding to interval 3) and *Schaubcylindrichnus* (ichnofabrics 9 and 6), which were not detected in the outcrops; b) trace fossils of centimetric size are only practically visible in outcrops and hardly detected in the core, i.e., *Cheiichnus* isp., *Gyrolithes variabilis* or *Thalassinoides suevicus*; c) field observations allow different ichnospecies to be discerned by their ornamentation or the presence of bioglyphs, features that are almost imperceptible in the sections of the core. This is the case of *Diplocraterion paralelum*, *Palaeophycus striatus*, *P. tubularis*, *Phycodes palmatus*, *Ph. ungulatus*, *Spongeliomorpha chevronensis*, *S. sinuostriata*, *Taenidium* isp., and *Teichichnus rectus;* and finally, d) bioerosional structures such as *Gastrochaenolites* isp., recorded in some burrows (*Thalassinoides* isp.) or in crusts, are not detected in the core.

In conclusion, if we consider the record of ichnotaxa only from the core analysis, just over 70% of the ichnotaxa actually differentiated would be obtained, since analysis in the field shows the existence of 16 ichnotaxa as opposed to 10 detected in the core. However, taking into account the information provided by the core and the field gives a total of 18 different ichnotaxa recorded.

A comparison of other ichnofabric features (Fig. 12) such as color, mottling, iron oxides, sedimentary structures and Bioturbation Index (B.I.) leads to several relevant observations. Color differences are not very significant, but in the field the white or gray tones predominate over pale yellow, the latter being more frequent in core ichnofabrics —but this is probably due to the higher degree of precision. Something similar occurs with the mottled background, usually showing a good correspondence, though in some cases, outcrop observations reveal a sparse presence that is not observed in the core (i.e., ichnofabrics 8 to 10 corresponding to intervals 3 to 5). This is probably due to the limited size of the core, which may penetrate an area of sparsely mottled sediment precisely there where it is not present. Iron oxides also present similarities between the two approaches. Generally, areas of sediment highly ferruginized in the core correspond to the presence of notorious ferruginous crusts in the field, yet some of the crusts observed in outcrop were not detected in the core (i.e., ferruginous crust located in the transition between intervals 7 and 8 is not observed in ichnofabric 5) or present just a punctual ferruginization. The most plausible explanation is that some of these crusts may have a reduced lateral extension, meaning the core does not cross them. Sedimentary structures observed in core and field are similar, although the core provides the most detailed and accurate view. As for the Bioturbation Index, observations in the field are quite approximate to those made for the core, even though, as in the previous case, the degree of accuracy is much higher in the core.

5. Discussion

5.1. Environmental setting and the involved paleoenvironmental conditions

Mayoral and Muñiz (2001a) established for this unit in Cabezo de La Zarcilla section a thickness of 12 to 14 m, while Muñiz et al. (2010) report 7 m and Belaústegui et al. (2016) figure just 4.5 m of thickness (figure 1 C, pag. 81); still, in the text they note that it can reach up to 14 m. It must be emphasized that these thicknesses are field data, as Mayoral et al. (2016) mention that recent cores in the area (Rodríguez-Tovar et al., 2013) give at least 30 m thick more. Further, still unpublished geophysical data place the contact with the Paleozoic basement at a depth of at least 130 m (Alonso Chaves, personal communication, Huelva University; research in progress). This implies that during the Miocene, the Lepe sector probably operated as a sub-basin isolated from the rest of the Guadalquivir Basin by a paleorelief of tectonic origin that would have been located more toward the East, in the area of Cartaya (8 km from Lepe).

In general, according to both ichnofabrics (*Ophiomorpha-Thalassinoides-Spongeliomorpha* and *Palaeophycus-Planolites-Phycosiphon* ichnofabrics) differentiated in outcrop, a continuous siliciclastic sedimentation can be interpreted, probably with low depositional energy, as supported by the presence of parallel lamination and the absence of significant discontinuity surfaces related to erosive processes. This sedimentation must be low to allow the maintenance of a well-developed and diverse macroinvertebrate trace maker community, associated with favorable paleoenvironmental parameters such as aerobic conditions and nutrient availability. However, the variable record of mottled background could reflect variations in the rate of sedimentation, sometimes high enough to impede rapid and complete colonization by trace makers. Punctually, an increase in energy conditions may be revealed by local low-angle cross-lamination. Most of the differentiated ichnotaxa can be associated with softground, but punctually looseground and even firmground could develop, as shown by the

record of *Ophiomorpha* and *Spongeliomorpha*, respectively. The fact that both ichnotaxa, together with *Thalassinoides*, are registered in the same interval 6, could have to do with lateral variations in consistency, rather than temporal changes. Bioerosive structures as *Gastrochaenolites* suggest firmer substrates. Organic material is mainly concentrated in the first few centimeters of the substrate, where the rate of oxygenation would be also higher, as indicated by the higher bioturbation found in shallower tiers. *Thalassinoides* isp., and *Ophiomorpha nodosa* reach lower levels of occupation, the corresponding trace makers being those that show greater exploitation capacity and reworking of sediments.

Lateral variations in paleoenvironmental conditions are also supported by the registered ichnoassociations. The recurring presence of the ichnotaxa identified in the field in different ichnocoenoses points to the existence of two ichnoassociations in the study area. The lower and upper part of the series (intervals 1-2 and 7-8) are characterized by the *Ophiomorpha-Thalassinoides* ichnoassociation (with *Spongeliomorpha* subordinate), while the middle part (interval 3-6) is characterized by the *Spongeliomorpha-Thalassinoides* ichnoassociation (with *Ophiomorpha, Phycodes* and *Planolites* subordinate). These data contrast with the observations by Muñiz (1998) and Muñiz et al. (1998) in La Zarcilla area, where, as mentioned above, three ichnoassociations were differentiated: *Ophiomorpha-Skolithos* (with *Thalassinoides* subordinate) for the lower part of the series; the *Gyrolithes variabilis* (accompanied by most of the ichnogenera mentioned above) for the middle part; and *Spongeliomorpha-Teichichnus-Phycodes* for the upper part. These differences in ichnoassociations for the same sedimentary unit reveals that, in the context of similar general paleoenvironmental conditions, local variations can modify the final record of bioturbation structures. Accordingly, the Lepe sector most likely operated as a sub-basin isolated from the rest of the Guadalquivir Basin by a paleorelief of tectonic origin, which could have determined local variations in the depositional environment and therefore in

the associated paleoenvironmental conditions. More specific, detailed analyses are required to constrain the above conditions and in particular their temporal evolution.

5.2. Sequence stratigraphy framework: A more detailed proposal

As underlined by Catuneanu et al. (2011), sequence stratigraphy is a conceptual revolution within the broad field of sedimentary geology, revamping the methodology of stratigraphic analysis. Characterizing the sequence stratigraphy framework is no easy matter, however, especially in cases where changes in facies or the geometric character of strata are not significant, key surfaces are difficult to recognize, and/or biostratigraphic control is deficient. This would be the case of the studied interval. Yet ichnological analysis has recently been revealed as a very useful aid in applied stratigraphy, sequence stratigraphy or genetic stratigraphy, helping to establish discontinuities and genetically related sedimentary packages in the fossil record (e.g., Pemberton and MacEachern, 1995, 2005; Pemberton et al., 2004; MacEachern et al., 2007a, b, 2012; Rodríguez-Tovar, 2010). This approach has been applied successfully in several outcrops from the Betic Cordillera (Olóriz and Rodríguez-Tovar, 2000; Olóriz et al., 2004; Rodríguez-Tovar et al., 2007; Rodríguez-Tovar and Nieto, 2013; Nieto et al., 2014), though an integrative outcrop plus core ichnofabric analysis has never been documented.

The Miocene succession studied here corresponds to a generalized transgression during the Tortonian, that in the sub-basin of Lepe was dominantly silty, in a marine infralittoral setting, probably a confined, subsiding bay affected by periodical small eustatic pulses related to tectonic movement of the paleorelief. In closed areas around the Guadalquivir Basin, a sequence stratigraphic framework has been established for the Tortonian-Messinian (Sierro et al., 1996; Ledesma, 2000; Abad, 2010). The proposal includes a transgressive system tract developed

during the Late Tortonian, corresponding to the sand and gravels from the Niebla Formation in the Cartaya-Huelva sector, and an extended high stand system tract developed during the Messinian p.p., corresponding to several units, consisting of with silts and calcareous silty clays, calcareous clays (Gibraleón Formation), and sand, silty sand and silts (Trigueros sands) (figure 3 in Salazar et al., 2016). A direct correlation of this proposal with the studied succession was initially difficult due to the absence of a detailed biostratigraphy that would have clearly discerned the Tortonian/Messinian boundary, so that the assignation of the studied section to the uppermost Tortonian-lowermost Messinian interval was deemed more appropriate. Still, the conducted research leads us to propose a general sequence stratigraphic framework, and even to improve on previous proposals by providing a more detailed characterization.

5.2.1. Sea-level changes: Low-frequency vs high-frequency processes

Ichnofabric distribution in outcrop at the long-scale shows the presence of the *Ophiomorpha-Thalassinoides-Spongeliomorpha* ichnofabric characterizing the lower and the upper part of the section (intervals 1-2 and intervals 6 to 8), and the *Palaeophycus-Planolites-Phycosiphon* ichnofabric restricted to the middle part (intervals 3-5). Two parts with a higher concentration of ferruginous crusts are registered, the first related to intervals 3 and 4, where ferruginous material and crusts are frequent, and the second in the upper part of the section, at the top of interval 7, in both cases associated with a higher Bioturbation Index (2 and 3). The *Palaeophycus-Planolites-Phycosiphon* ichnofabric, hence intervals 3 to 5, are also characterized by sparse mottling that appears gradually in the interval below and disappears gradually in the one above characterized by no mottled field observations. Intervals 3 to 5 furthermore show the presence of *Gastrochaenolites* isp. With respect to the tiering structure, shallower levels present a higher degree of occupation, and unlike the other ichnofabric, *Thalassinoides, Ophiomorpha*

and *Spongeliomorpha* are rarely found below 50 cm depth. Intervals 3 to 5 are also characterized by the presence of horizontal lamination.

With respect to core Lepe S1, the section studied in outcrop (around 13.5 m) is included in the upper part of the core (from meter 20.6 to the top; Fig. 10), corresponding particularly to the top of its lower half (from meter 13.5 to meter 12). This upper part is characterized by the presence of coarser ichnofabrics (ichnofabric 14), and its entire upper half, in turn (from meter 12 to meter 0), shows a dominance of non-mottled fine to medium grained ichnofabrics (ichnofabrics 9 and 11). Coinciding with the record of *Palaeophycus-Planolites-Phycosiphon* ichnofabric in outcrop (intervals 3 to 5), the core record reveals a higher abundance of ferruginization, as well as a comparatively high Bioturbation Index (2 to 3).

In a context of mainly siliciclastic sedimentation, the finer grained sediments registered in intervals 2 to 5 (outcrop and core), associated with greater ferruginization, including ferruginous crust (outcrop and core), the presence of sparse mottling (outcrop), a higher Bioturbation Index (outcrop and core), and the punctual record of *Gastrochaenolites* isp. (outcrop), could mark a significant change in depositional conditions, from below and above. Lesser depositional energy, and a lower rate of sedimentation, could mean more time for trace maker activity, favoring ferruginization and bioturbation especially in shallower tiers. These changes could correspond to the final transgressive system tract. This interval in particular could be interpreted as the "condensed deposits" accumulated during the time of maximum transgression, with the maximum flooding surface evidenced by the point of highest Bioturbation Index and interpreted as indicative of the change from transgression to highstand normal regression (Catuneanu, 2006; Catuneanu et al., 2009, 2011; Catuneanu and Zecchin, 2013; Zecchin and Catuneanu, 2013, 2015 and references therein). However, we have no physical expression of a unique and significant flooding surface reflecting the maximum flooding event,

making it preferable to interpret the entire package of intervals 3 to 5 as the "maximum flooding zone", characterized by greater bioturbation (Zecchin and Catuneanu, 2013 and references therein). As these authors indicate, transgressive deposits may gradually give rise to regressive ones without significant sediment starvation.

In such a context, the studied succession would correspond to the development of the final phases of a transgressive system tract (intervals 1 and 2), the "maximum flooding zone" (mainly intervals 3 to 5), and then the highstand normal regression (intervals 6 to 8). This proposal fits with the one expounded above.

Notwithstanding, within this overall long-term sequence stratigraphy pattern, the short-term ichnofabric trends registered in the core could serve to refine the proposal at a high-frequency scale of the processes involved. Thus, the upper half of the section in core (from meter 12 to meter 0) shows two clearly different parts: a) the lower one, correlated with intervals 3 to 5 and 6 p.p., displays well-defined, numerous, and thin alternations mainly involving ichnofabrics 6, 8 and 9, with transitions mainly between ichnofabrics 6 and 8 (below) and 9 (above); and b) the upper part, from interval 6 p.p. to interval 8, shows a less evident alternation pattern yet a dominance of thick ichnofabric 11. The well-defined alternation pattern of the lower part is associated with high ferruginization atop each alternation, as well as an increase in the Bioturbation Index. In a "maximum flooding zone" scenario, the high-frequency repetitive pattern involving ichnofabric 9 on top, linked with the record of high ferruginization and even ferruginized crust, could mark "local flooding surfaces" (LSF; Abbott and Carter, 1994 in Zecchin and Catuneanu, 2013) revealing facies contacts within transgressive system tracts. According to Zecchin and Catuneanu (2013), LSF may be characterized by intense burrowing (*Glossifungites* ichnofacies); in our case study a well-developed *Glossifungites* ichnofacies is not clearly defined, but the local presence of bioerosion structures such as *Gastrochaenolites*

exclusively in some of the ferruginous crusts would agree with this interpretation. The interpreted LFS could therefore correspond to boundaries of parasequences within the "maximum flooding zone", capping alternations of small sedimentary packages starting with ichnofabric 6 or 11 and ending in ichnofabric 9.

6. Conclusions

Ichnofabric analysis conducted in Miocene sediments from Lepe (Huelva, SW Spain) reveals the usefulness of integrative studies that include outcrop and core information, in order to improve interpretations of depositional and paleoenvironmental conditions, with special attention to the sequence stratigraphy framework.

Outcrop research based on stratigraphic and ichnological features allowed us to differentiate two ichnofabrics. *Ophiomorpha-Thalassinoides-Spongeliomorpha* ichnofabric was identified for study intervals 1, 2, 6, 7 and 8, and *Palaeophycus-Planolites-Phycosiphon* ichnofabric for intervals 3, 4 and 5. In turn, core analysis, mainly based on lithological features —including ferruginous material, grain size, mottled background, ichnotaxa, and Bioturbation Index— allowed for the characterization of fourteen ichnofabrics.

The comparison between outcrop and core ichnofabrics, conducted in the upper 13.5 m, corresponding to the uppermost Tortonian-Lowermost Messinian interval, reveals noteworthy similarities as well as some differences between the two records.

A continuous siliciclastic deposition, with punctual variations in the rate of sedimentation, must be interpreted, along with aerobic conditions and nutrient availability, allowing a well-developed and diverse macroinvertebrate trace maker community to be

maintained. Softgrounds were dominant, but punctually loosegrounds and firmgrounds developed.

Long-scale patterns in the distribution of ichnofabrics from outcrop and core suggest the last phases of a transgressive system tract, with a "maximum flooding zone" at the end, and then the highstand normal regression. High-frequency, short-scale, repetitive patterns in ichnofabrics from core, mainly between ichnofabrics 6 and 8 (below) and 9 (above), may be related to "local flooding surfaces", subdividing the "maximum flooding zone" into parasequences.

Acknowledgements

Funding for this research was provided by Project CGL2015-66835-P (Secretaría de Estado de I+D+I, Spain), and Research Groups RNM-178 and RNM-276 (Junta de Andalucía). The research of JD was financed with a pre-doctoral grant supported by the University of Granada.

References

Abad, M., 2010. La transgresión tortoniense en el margen pasivo de la cuenca del Guadalquivir: respuesta estratigráfica e implicaciones paleontológicas. Ph.D. thesis, University of Huelva, Spain.

Abad, M., Muñiz, F., Toscano, A., Izquierdo, T., Ruiz, F., 2013. Significance of hummocky cross-stratification in a coastal succession of the Western Guadalquivir Basin (Upper Neogene, SW Spain). V RCANS Congress Abstract Book, University of Huelva, Spain.

Abbott, S.T., Carter, R.M., 1994. The sequence architecture of mid-Pleistocene (c.1.1.-0.4 Ma)

cyclothems from New Zealand: facies development during a period of orbital control on sea-level cyclicity. In: De Boer, P.L., Smith, D.G. (Eds.), Orbital Forcing and Cyclic Sequences. International Association of Sedimentologists Special Publication 19, pp. 367−394.

Belaústegui, Z., Muñiz, F., Mángano, M.G., Buatois, L.A., Domènech, R., Martinell, J., 2016. *Lepeichnus giberti* igen. nov. isp. nov. from the upper Miocene of Lepe (Huelva, SW Spain): Evidence for its origin and development with proposal of a new concept, ichnogeny. Palaeogeography, Palaeoclimatology, Palaeoecology 452, 80−89.

Buatois, L.A., Mángano, M.G., 2011. Ichnology: Organism-Substrate Interactions in Space and Time. Cambridge University Press, New York.

Catuneanu, O., 2006. Principles of Sequence Stratigraphy. Elsevier, Amsterdam.

Catuneanu, O., Zecchin, M., 2013. High-resolution sequence stratigraphy of clastic shelves II: controls on sequence development. Marine and Petroleum Geology 39, 26−38.

Catuneanu, O., Abreu, V., Bhattacharya, J.P., Blum, M.D., Dalrymple, R.W., Eriksson, P.G., Fielding, C.R., Fisher, W.L., Galloway, W.E., Gibling, M.R., Giles, K.A., Holbrook, J.M., Jordan, R., Kendall, C.G.St.C., Macurda, B., Martinsen, O.J., Miall, A.D., Neal, J.E., Nummedal, D., Pomar, L., Posamentier, H.W., Pratt, B.R., Sarg, J.F., Shanley, K.W., Steel, R.J., Strasser, A., Tucker, M.E., Winker, C., 2009. Towards the standardization of sequence stratigraphy. Earth-Science Reviews 92, 1−33.

Catuneanu, O., Galloway, W.E., Kendall, C.G.St.C., Miall, A.D., Posamentier, H.W., Strasser, A., Tucker, M.E., 2011. Sequence stratigraphy: methodology and nomenclature. Newsletters on Stratigraphy 44 (3), 173−245.

694 Dorador, J., Rodríguez-Tovar, F.J., 2016. Stratigraphic variation in ichnofabrics at the
695 "Shackleton Site" (IODP Site U1385) on the Iberian Margin: Paleoenvironmental
696 implications. Marine Geology 377, 118–126.

697 Ekdale, A.A., Bromley, R.G., Knaust, D., 2012. The Ichnofabric Concept. In: Knaust, D.,
698 Bromley, R.G. (Eds.), Trace Fossils as Indicators of Sedimentary Environments.
699 Developments in Sedimentology 64. Elsevier, Amsterdam, pp. 139–155.

700 Gámez-Vintaned, J.A., Mayoral Alfaro., E., 1992. Primeras aportaciones a la Paleoicnología del
701 Grupo Murero (Cámbrico inferior-medio) en Murero, Provincia de Zaragoza, Cadena
702 Ibérica Occidental. Geogaceta 12, 100–102.

703 Knaust, D., Bromley, R.G., 2012. Trace Fossils as Indicators of Sedimentary Environments.
704 Developments in Sedimentology 64. Elsevier, Amsterdam.

705 Ledesma, S., 2000. Astrobiocronología y estratigrafía de alta resolución del Neógeno de la
706 Cuenca del Guadalquivir-Golfo de Cádiz. Ph.D. thesis, University of Salamanca.

707 MacEachern, J.A., Gingras, M.K., Bann, K.L., Pemberton, S.G., Dafoe, L.T., 2007a.
708 Applications of ichnology to high-resolution genetic stratigraphic paradigms. In:
709 MacEachern, J.A., Bann, K.L., Gingras, M.K., Pemberton, S.G. (Eds.), Applied
710 Ichnology. SEPM Short Course Notes 52, pp. 95–129.

711 MacEachern, J.A., Pemberton, S.G., Gingras, M.K., Bann, K.L., Dafoe, L.T., 2007b. Use of trace
712 fossils in genetic stratigraphy. In: Miller III, W. (Ed.), Trace Fossils. Concepts, Problems,
713 Prospects. Elsevier, pp. 105–128.

MacEachern, J.A., Dashtgard, S.E., Knaust, D., Catuneanu, O., Bann, K.L., and Pemberton, S.G. 2012. Sequence Stratigraphy. In: Knaust, D., Bromley, R. (Eds.), Trace Fossils as Indicators of Sedimentary Environments. Developments in Sedimentology 64. Elsevier, Amsterdam, pp. 157–194.

Mayoral, E., Muñiz., F., 1994. Presencia de un nuevo Cefalópodo Sepioideo en el Neógeno superior de la Cuenca del Guadalquivir (Lepe, Huelva, España). Coloquios de Paleontología 46, 155–168.

Mayoral, E., Muñiz, F., 1995. Nueva icnoespecie de *Gyrolithes* del Mioceno Superior de la Cuenca del Guadalquivir (Lepe, Huelva). Revista Española de Paleontología 10(2), 190−201.

Mayoral, E., Muñiz, F., 1996. Tafonomía de las pistas fósiles y su aplicación en las reconstrucciones paleoambientales del neógeno marino de Lepe (Huelva). Comunicación de la II Reunión de Tafonomía y fosilización, 205−210.

Mayoral, E., Muñiz, F., 1998. Nuevos datos icnotaxonómicos sobre *Gyrolithes* del Plioceno inferior de la Cuenca del Guadalquivir (Lepe, Huelva, España). Revista Española de Paleontología 13(1), 61−69.

Mayoral, E., Muñiz, F., 2001. Ichnologie Note; New Ichnoespecies of *Cardioichnus* from the Miocene of the Guadalquivir Basin, Huelva, Spain. Ichnos 8(1), 69−76.

Mayoral, E., Salazar Rincón, A., Santos, A., 2016. Estratigrafía y Paleontología del Neógeno Superior en el sector suroccidental de la Cuenca del Guadalquivir. In: García Navarro, E., Cantano Martín, M., Morales González, J.A. (Eds.), Guía de Excursiones del IX

735 Congreso Geológico de España Huelva, pp. 1−54.

736 Muñiz, F., 1998. Paleoicnología del Neógeno superior en el sector suroccidental de la Cuenca del
737 Guadalquivir, área de Ayamonte (Huelva). Ph.D. thesis, University of Huelva.

738 Muñiz, F., Mayoral, E., 1999. Nueva pista fósil del Mioceno Superior en el sector suroccidental
739 de la Cuenca del Guadalquivir (Lepe, Huelva, España). Temas Geológico-Mineros ITGE
740 26, 276−279.

741 Muñiz, F., Mayoral, E., 2001a. *Macanopsis plataniformis* nov. ichnosp. from the Lower
742 Cretaceous and Upper Miocene of the Iberian peninsula. Geobios 34, 91–98.

743 Muñiz, F., Mayoral, E., 2001b. El icnogénero *Spongeliomorpha* en el Neógeno superior de la
744 Cuenca del Guadalquivir (área de Lepe–Ayamonte, Huelva, España). Revista Española
745 de Paleontología 16, 115–130.

746 Muñiz, F., Mayoral, E., Gámez Vintaned, J.A., 1998. Icnofacies del Neógeno superior de la
747 Cuenca del Guadalquivir (área de Lepe-Ayamonte, Huelva, España). Geogaceta 24,
748 235−238.

749 Muñiz, F., Mayoral, E., Cáceres, L.M., Cachão, M., 2001a. Nuevos datos bio-
750 cronoestratigráficos para el sector suroccidental de la cuenca del Guadalquivir (Área de
751 Lepe- Ayamonte, Huelva, España). Geogaceta 30, 243−244.

752 Muñiz, F., Mayoral, E., Cáceres, L.M., Cachão, M., 2001b. Correlación entre las unidades
753 litoestratigráficas del Neógeno superior en el sector suroccidental de la Península Ibérica.
754 Geogaceta 30, 239−241.

Muñiz, F., Belaústegui, Z., Cárcamo, C., Domènech, R., Martinell, J., 2015. *Cruziana*- and *Rusophycus*-like traces of recent Sparidae fish in the estuary of the Piedras River (Lepe, Huelva, SW Spain). Palaeogeography, Palaeoclimatology, Palaeoecology 439, 176−183.

Muñiz, F., de Gibert, J.M., Mayoral, E., Belaústegui, Z., 2010. Fieldtrip Guidebook of the Workshop on Crustacean Bioturbation – Fossil and Recent. University of Huelva.

Nieto, L.M., Rodríguez-Tovar, F.J., Molina, J.M., Reolid, M., Ruiz-Ortiz, P.A., 2014. Unconformity surfaces in pelagic carbonate environments: A case from the Middle Bathonian of the Betic Cordillera, SE Spain. Annales Societatis Geologorum Poloniae 84, 281–295.

Olóriz, F., Rodríguez-Tovar, F.J., 2000. *Diplocraterion*: a useful marker for sequence stratigraphy and correlation in the Kimmeridgian, Jurassic (Prebetic Zone, Betic Cordillera, southern Spain). Palaios 15, 546–552.

Olóriz, F., Reolid, M., Rodríguez-Tovar, F.J., 2004. Microboring and taphonomy in Middle Oxfordian to lowermost Kimmeridgian (Upper Jurassic) from the Prebetic Zone (southern Iberia). Palaeogeography, Palaeoclimatology, Palaeoecology 212, 181−197.

Pemberton, S.G., MacEachern, J.A., 1995. The sequence stratigraphic significance of trace fossils: examples from the Cretaceous foreland basin of Alberta, Canada. In: Van Wagoner, J.C., Bertram, G. (Eds.), Sequence Stratigraphy of Foreland Basin Deposits: Outcrop and Subsurface Examples from the Cretaceous of North America, AAPG Memorial Guidelines 64, pp. 429–475.

775 Pemberton, S.G., MacEachern, J.A., 2005. Significance of ichnofossils in applied stratigraphy.
776 In: Koutsoukos, E.A. (Ed.), Applied Stratigraphy. Springer, Netherlands, pp. 281–302.

777 Pemberton, S.G., MacEachern, J.A., Saunders, T.D.A., 2004. Stratigraphic applications of
778 substratespecific ichnofacies: delineating discontinuities in the rock record. In: McIlroy,
779 D. (Ed.), The Application of Ichnology to Palaeoenvironmental and Stratigraphic
780 Analysis. Geological Society, London, Special Publications 228, pp. 29–62.

781 Rodríguez-Tovar, F.J., 2010. Ichnological Analysis and Sequence Stratigraphy Research:
782 Present-Day and Prospective. Memoir Geological Society of India 75, 99–114.

783 Rodríguez-Tovar, F.J., Nieto, L.M., 2013. Composite Trace Fossil Assemblage in Distal
784 Carbonate Swell Settings from the Pelagic Tethyan Domain (Middle Jurassic, Betic
785 Cordillera, South ern Spain). Ichnos 20, 43–53.

786 Rodríguez-Tovar, F.J., Pérez-Valera, F., Pérez-López, A., 2007. Ichnological analysis in high-
787 resolution sequence stratigraphy: The *Glossifungites* ichnofacies in Triassic successions
788 from the Betic Cordillera (southern Spain). Sedimentary Geology 198, 293–307.

789 Rodríguez-Tovar, F.J., Dorador, J., Mayoral, E., Santos, A., 2013. Sedimentología e icnología
790 del sondeo S-0 (Mioceno superior de Lepe, Huelva). Two decades of Atlantic Neogene
791 study. V RCANS Congress Abstract Book, University of Huelva, Spain.

792 Salazar, A., Larrasoaña, J.C., Abad, M., Mayoral, E., Pérez-Asensio, J.N., González-Regalado,
793 M.L., Martín-Banda, R., Civis, J., Mata, M.P., 2016. Neogene lithological units at the
794 west end of Guadalquivir Basin and their correlations with the Huelva-1 borehole
795 (Huelva-Spain). Geo-Temas 16, 173–176.

796 Shepard, F. P., 1954. Nomenclature based on sand-silt-clay ratios. Journal Sedimentary
797 Petrology 24, 151–158.

798 Sierro, F.J., González Delgado, J.A, Dabrio, C., Flores J.A., Civis, J., 1996. Late Neogene
799 depositional sequences in the foreland basin of Guadalquivir (SW Spain). In: Friend, P.,
800 Dabrio, C. (Eds.), Tertiary basins of Spain. Cambridge University Press, Cambridge, pp.
801 339–345.

802 Taylor, A.M., Goldring, R., 1993. Description and analysis of bioturbation and ichnofabric.
803 Journal of Geological Society of London 150, 141–148.

804 Wentworth, C.K., 1922. A scale of grade and class terms for clastic sediments. Journal of
805 Geology 30, 377–392.

806 Zecchin, M., Catuneanu, O., 2013. High-resolution sequence stratigraphy of clastic shelves I:
807 Units and bounding surfaces. Marine and Petroleum Geology 39, 1–25.

808 Zecchin, M., Catuneanu, O., 2015. High-resolution sequence stratigraphy of clastic shelves III:
809 Applications to reservoir petrology. Marine and Petroleum Geology 64, 161-175.

810

811

812 **FIGURE CAPTIONS**

813

814 **Fig. 1.** Geographic and geological location of the studied area and borehole Lepe S1.

815 **Fig. 2.** General stratigraphic log of the section studied in outcrop and location of borehole

816 Lepe S1.

817 **Fig. 3.** A) Driller Rolatec RL 48 L used to retrieve the study core (Lepe S1). B) Sections

818 of core Lepe S1 at the laboratory of the Department of Stratigraphy and Palaeontology

819 (University of Granada).

820 **Fig. 4.** Distribution of differentiated ichnotaxa in core (column A, variable colors) and

821 outcrop (column B, gray tone). Numbers in column A correspond to ichnofabrics in core and in

822 column B to intervals in outcrop. For more details see text.

823 **Fig. 5.** Tiering and characteristic ichnofabrics deduced from the outcrop analysis. A)

824 *Ophiomorpha-Thalassinoides-Spongeliomorpha* ichnofabric. B) *Palaeophycus-Planolites-*

825 *Phycosyphon* ichnofabric. Legend for ichnotaxa: Ch: *Cheiichnus* isp., Co: *Conichnus* isp., D:

826 *Diplocraterion paralellum*, G: *Gyrolithes variabilis*, On: *Ophiomorpha nodosa*, Op:

827 *Ophiomorpha* isp., Pa: *Palaeophycus* isp., Ps: *Palaeophycus striatus*, Pt: *Palaeophycus tubularis*,

828 Pl: *Planolites* isp., Pdp: *Phycodes palmatus*, Pdu: *Phycodes ungulatus*, Phy: *Phycosiphon* isp.,

829 Ro: *Rosselia* isp., Sk: *Skolithos* isp., Sch: *Spongeliomorpha chevronensis*, Ss: *Spongeliomorpha*

830 *sinuostriata*, Ta: *Taenidium* isp., Te: *Teichichnus* isp., Tr: *Teichichnus rectus*, Th:

831 *Thalassinoides* isp., Ths: *Thalassinoides suevicus*.

832 **Fig. 6.** General views of the ichnofabrics in the field according to differentiated intervals.

833 A-C – *Palaeophycus-Planolites-Phycosiphon* ichnofabric. A) Interval 3. Pl: *Planolites* isp., Te:

834 *Teichichnus* isp., Phy: *Phycosiphon*. B) Interval 4. Pl: *Planolites* isp., Te: *Teichichnus* isp., Th:

Thalassinoides isp. C) Interval 5. Sparsely mottled silts with small disperse *Phycosiphon* isp. D) *Ophiomorpha-Thalassinoides-Spongeliomorpha* ichnofabric. Interval 6. Mottled sandy silts with large *Thalassinoides* isp. E) Panoramic view of intervals 4 and 5. F) Panoramic view of intervals 6 and 7.

Fig. 7. Trace fossils observed in outcrop. A) *Phycodes palmatus*. Interval 4. Scale bar: 6 cm. B-C – *Rosselia* isp. Interval 2. B) Lateral view. C) Plant view. Scale bar: 1 cm. D)*Ophiomorpha nodosa* (On) and *Ophiomorpha* isp. (Op) in plant view. Top of the interval 1. Scale bar: 5 cm. E-F – *Gastrochaenolites* isp. E) on *Thalassinoides* isp. Interval 3. Scale bar: 1 cm. F) on ferruginous crust. Interval 4. Scale bar: 5 cm. G-H – *Teichichnus rectus*, Interval 4. G) Lateral view. H) Transversal section. Scale bar for both: 1 cm. I – *Cheiichnus* isp. Interval 7. Scale bar: 1 cm. J – *Conichnus* isp. Interval 7. Scale bar: 1 cm. K – *Spongeliomorpha sinuostriata*. Interval 3. Scale bar: 10 cm. L – *Thalassinoides* isp., and *Planolites* isp. (Pl). Interval 6. Scale of the hoe head: 12 cm. M – *Palaeophycus tubularis*. Interval 7. Scale bar: 1 cm. N – *Taenidium* isp. Interval 3. Scale bar: 4 cm. O – *Gyrolithes variabilis*. Interval 8. Scale bar: 5 cm. P – *Ophiomorpha nodosa*. Interval 7. Scale bar: 1 cm. Q – *Palaeophycus* isp. Interval 3. Scale bar: 1 cm.

Fig. 8. Close-up illustration of the differentiated ichnofabrics in core Lepe S1, showing some of the characteristic features. Note: dlis: drilling lamination induced structures, G: *Gyrolithes*, Ma: *Macaronichnus*, Op: *Ophiomorpha*, ?Pd: ?*Phycodes*, Pl: *Planolites*, Sch: *Schaubcylindrichnus*, Te: *Teichichnus*, Th: *Thalassinoides*.

Fig. 9. Relative abundances of the individual differentiated ichnofabrics (1 to 14) in core Lepe S1, as well as grouped according to grain size. Note that iron crusts are included.

Fig. 10. Stratigraphic distribution of the differentiated ichnofabrics (1 to 14) throughout the entire core Lepe S1 (around 37.5 m-thick). In gray the section of the core (around 13.5 m-thick) compared with outcrop in Figures 4 and 12.

Fig. 11. Relative abundance of ichnofabrics in core Lepe S1, with differentiation between lower (bottom to around 21 m in depth) and upper (around 21 m in depth to top) parts.

Fig. 12. Comparison of the parameters characterizing the ichnofabrics observed in the core and in the field. Column A: Numbers inside correspond to the ichnofabrics in core. Column B: Ichnofabrics in field. For more details see text.

868 **TABLE CAPTIONS**

869

870 **Table 1.** Differentiated ichnofabrics in core Lepe S1 (1 to 14) with relevant features.

871

872 **Table 2.** Transitions (in %) between the differentiated ichnofabrics characterized in
873 correlative 10 cm-thick intervals. Percentage refers to the times that one ichnofabric (column)
874 transits to another one (row), from bottom to top. In italics, the values corresponding to
875 ichnofabrics recognized only in the lower part, and non-italics those recognized in the upper one.
876 Column 15 (values in gray) represents iron crust, identified in both halves.

Figure 1
Click here to download high resolution image

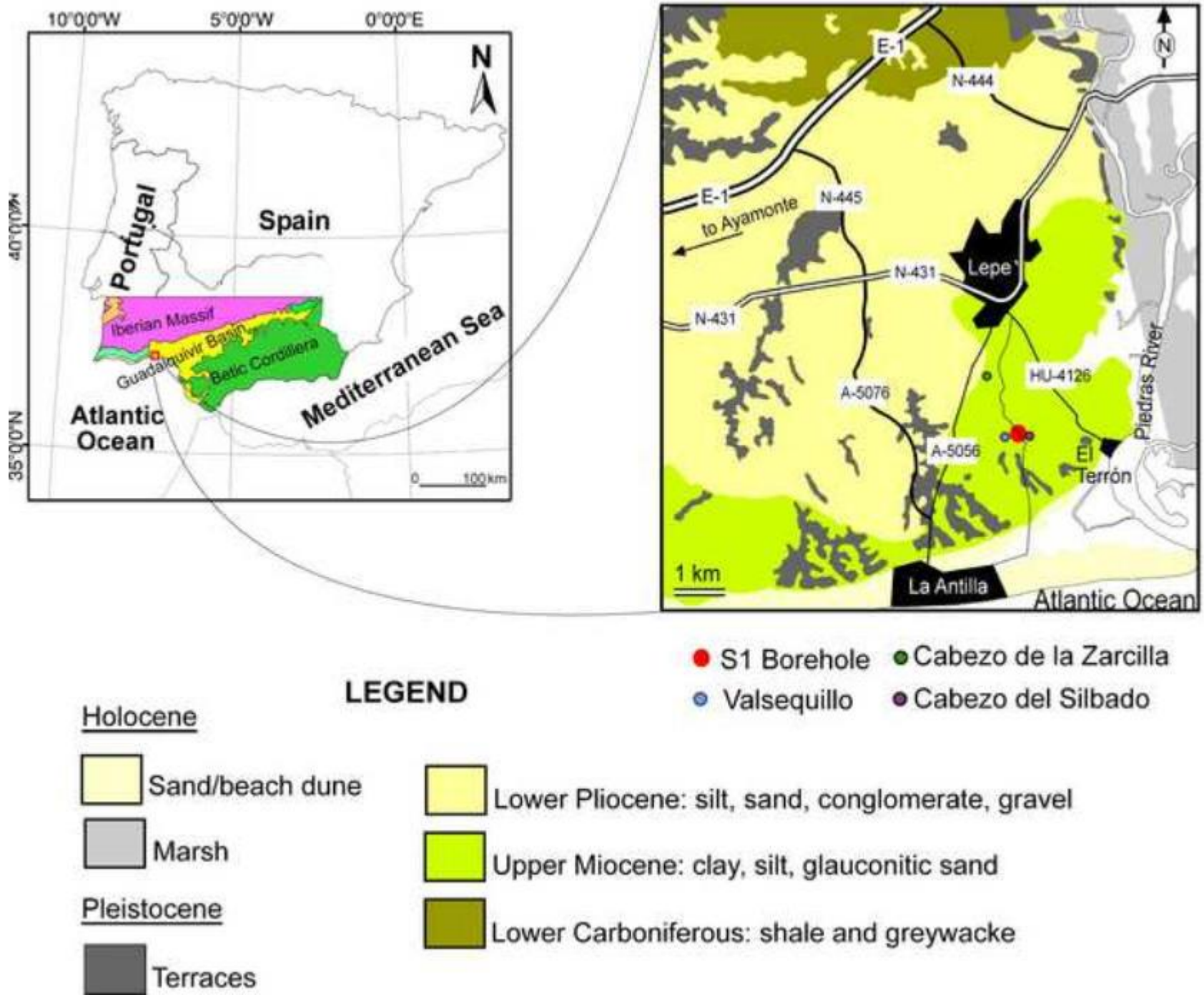

Figure 2
Click here to download high resolution image

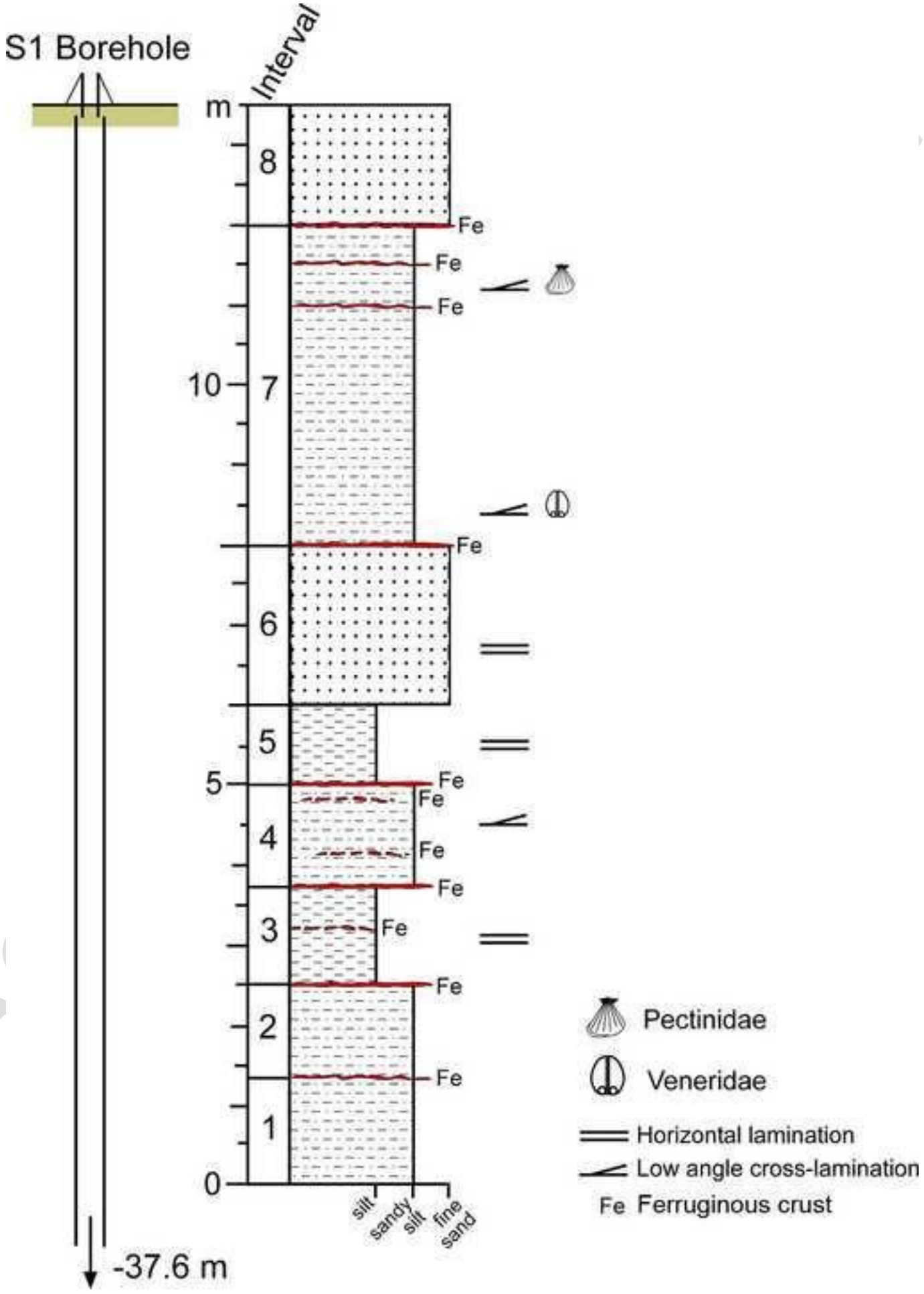

Figure 3
Click here to download high resolution image

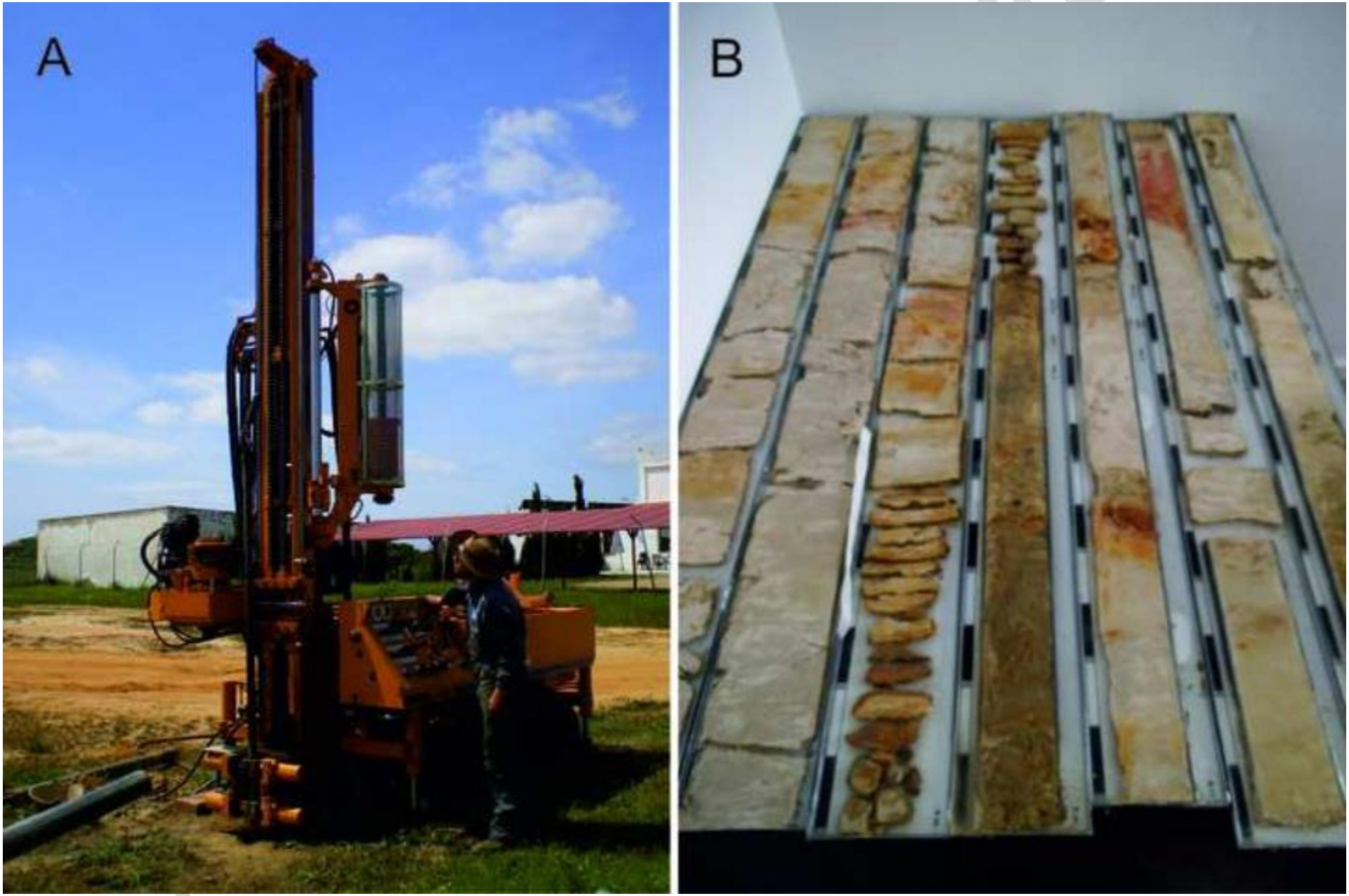

Figure 4

Click here to download high resolution image

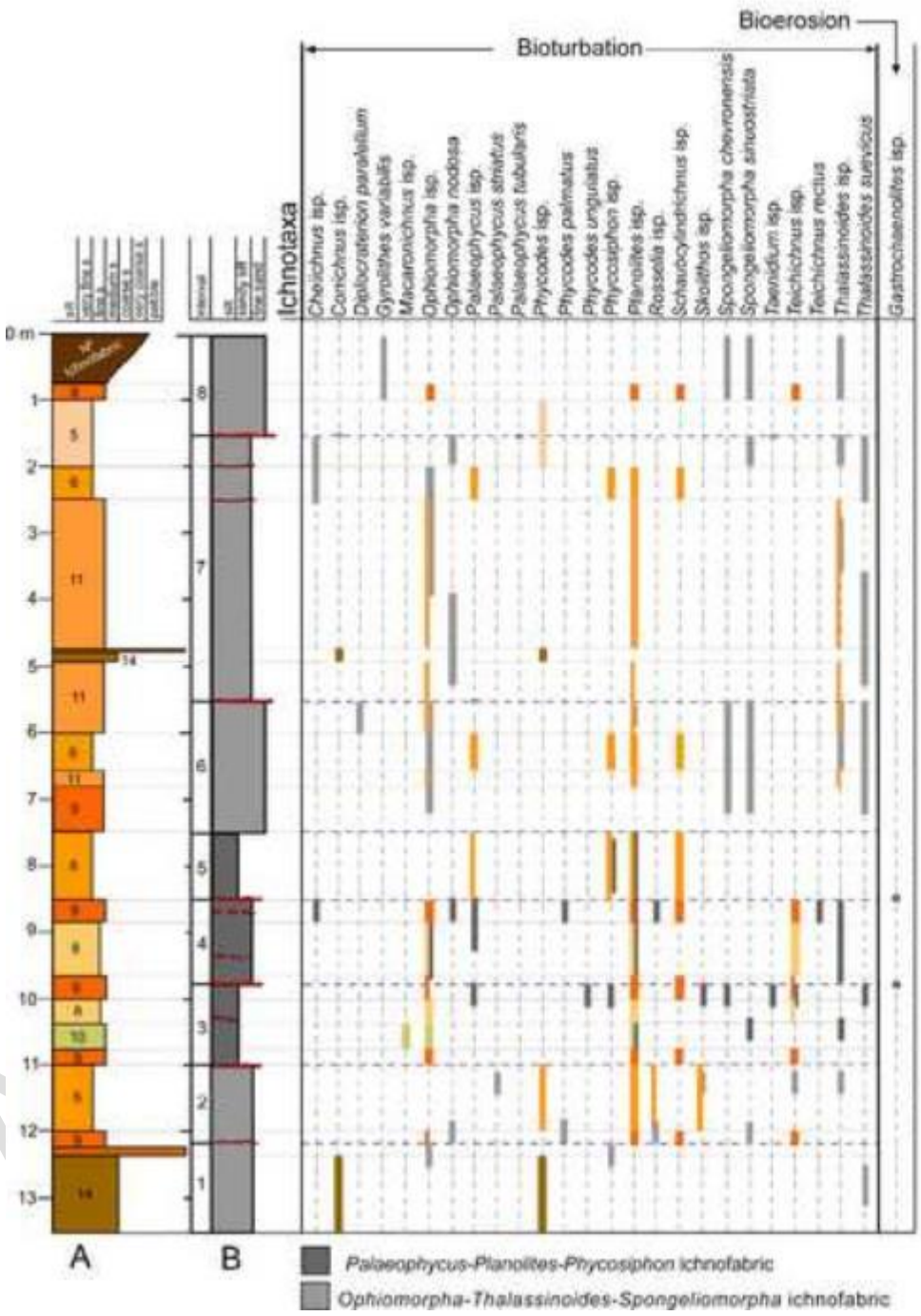

Figure 5
Click here to download high resolution image

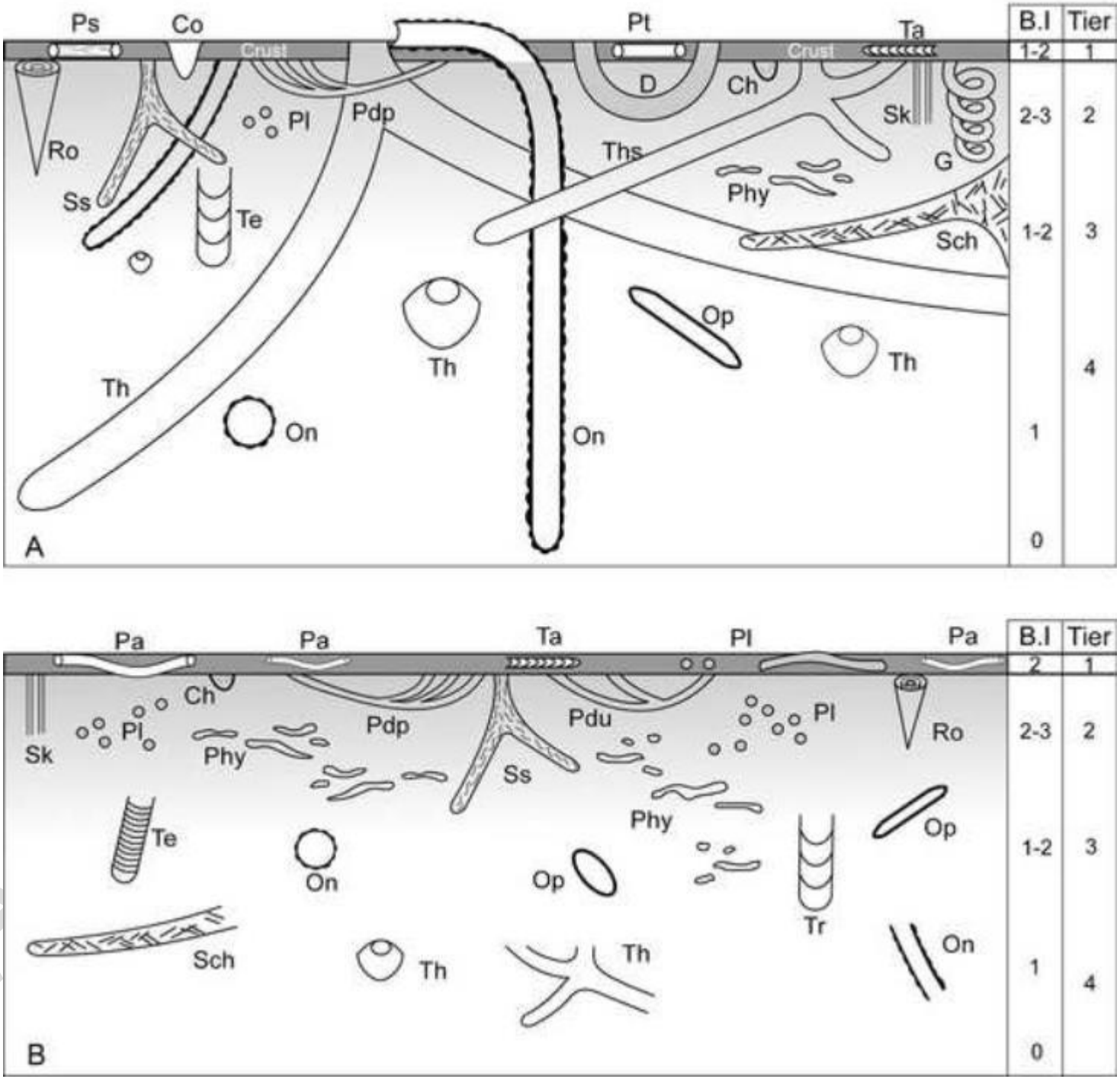

Figure 6

Click here to download high resolution image

Figure 7
Click here to download high resolution image

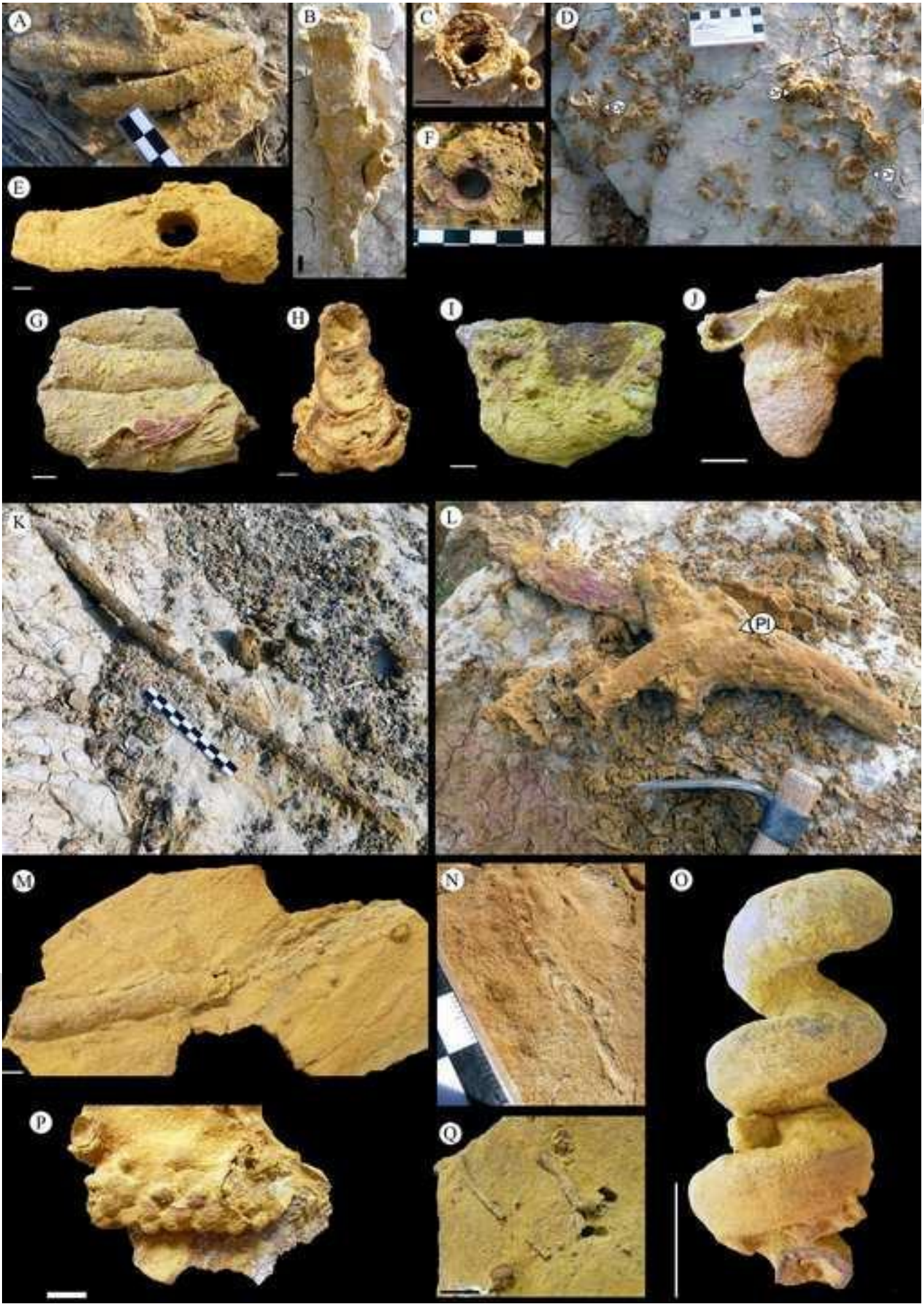

Figure 8

Click here to download high resolution image

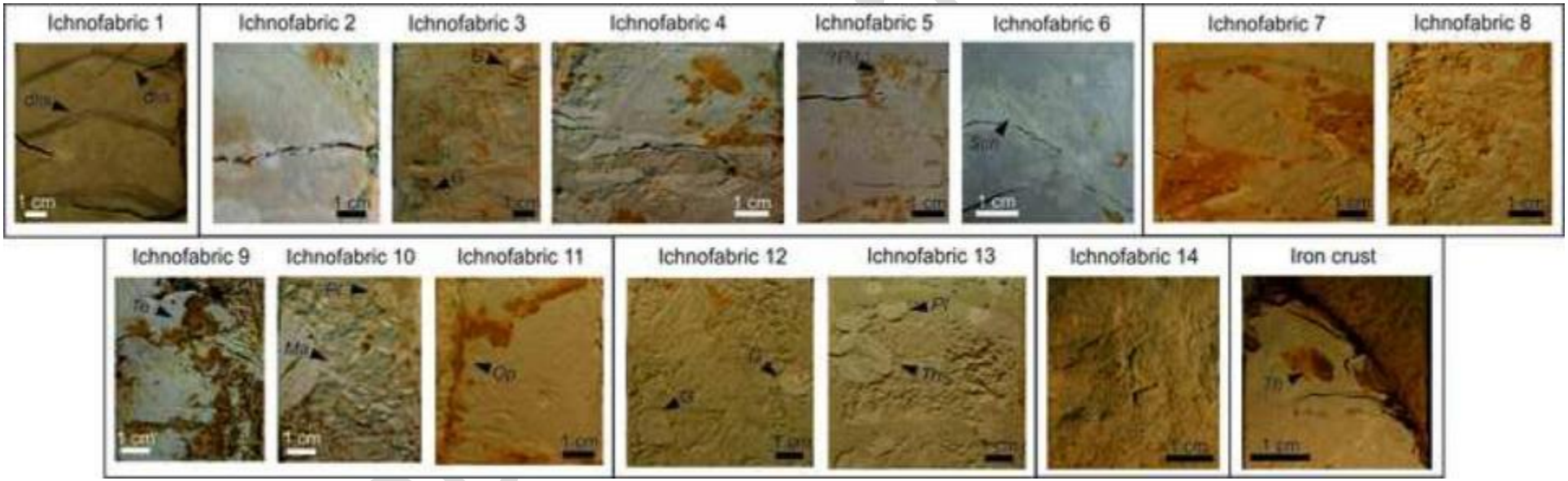

Figure 9
Click here to download high resolution image

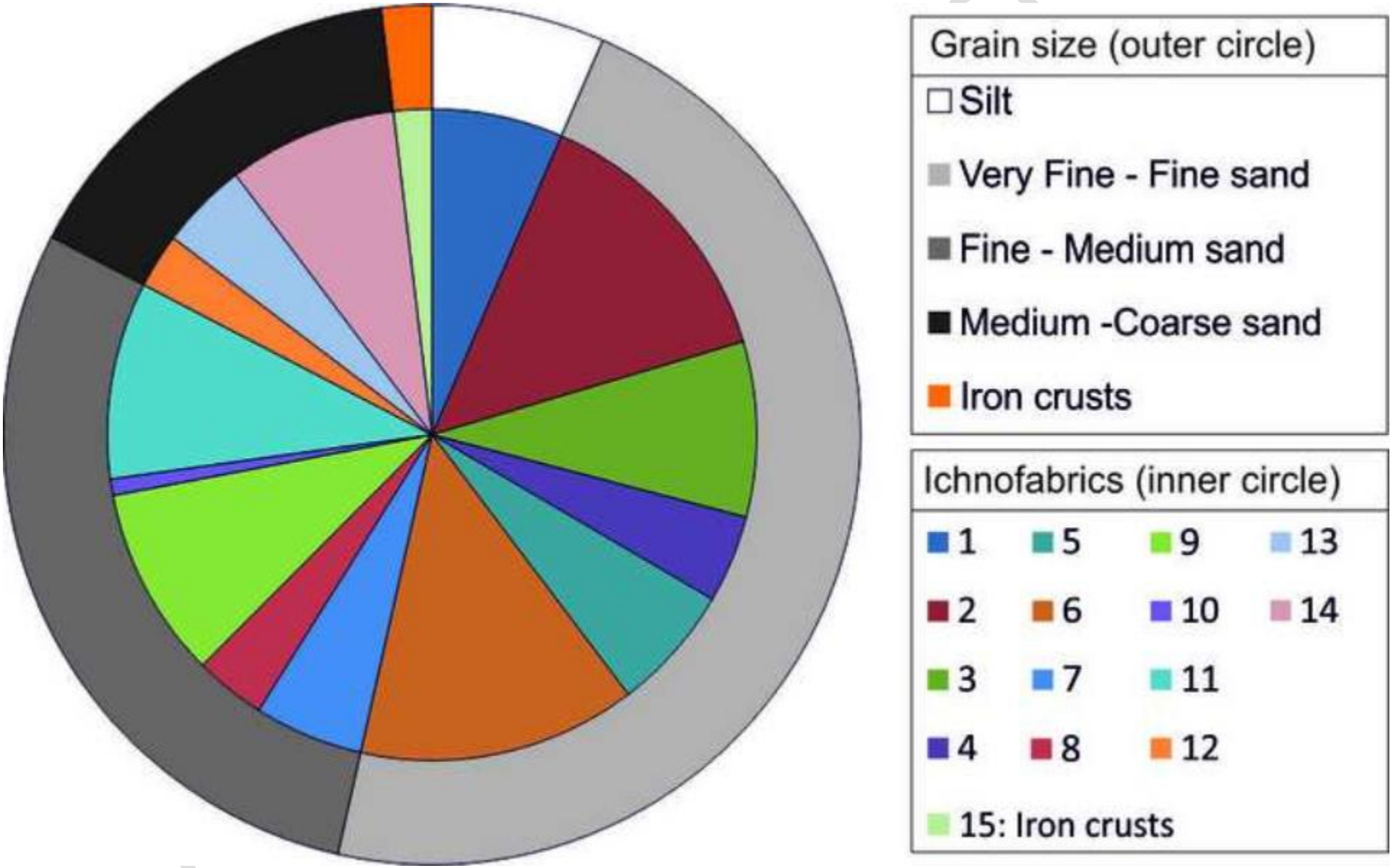

Figure 10

Click here to download high resolution image

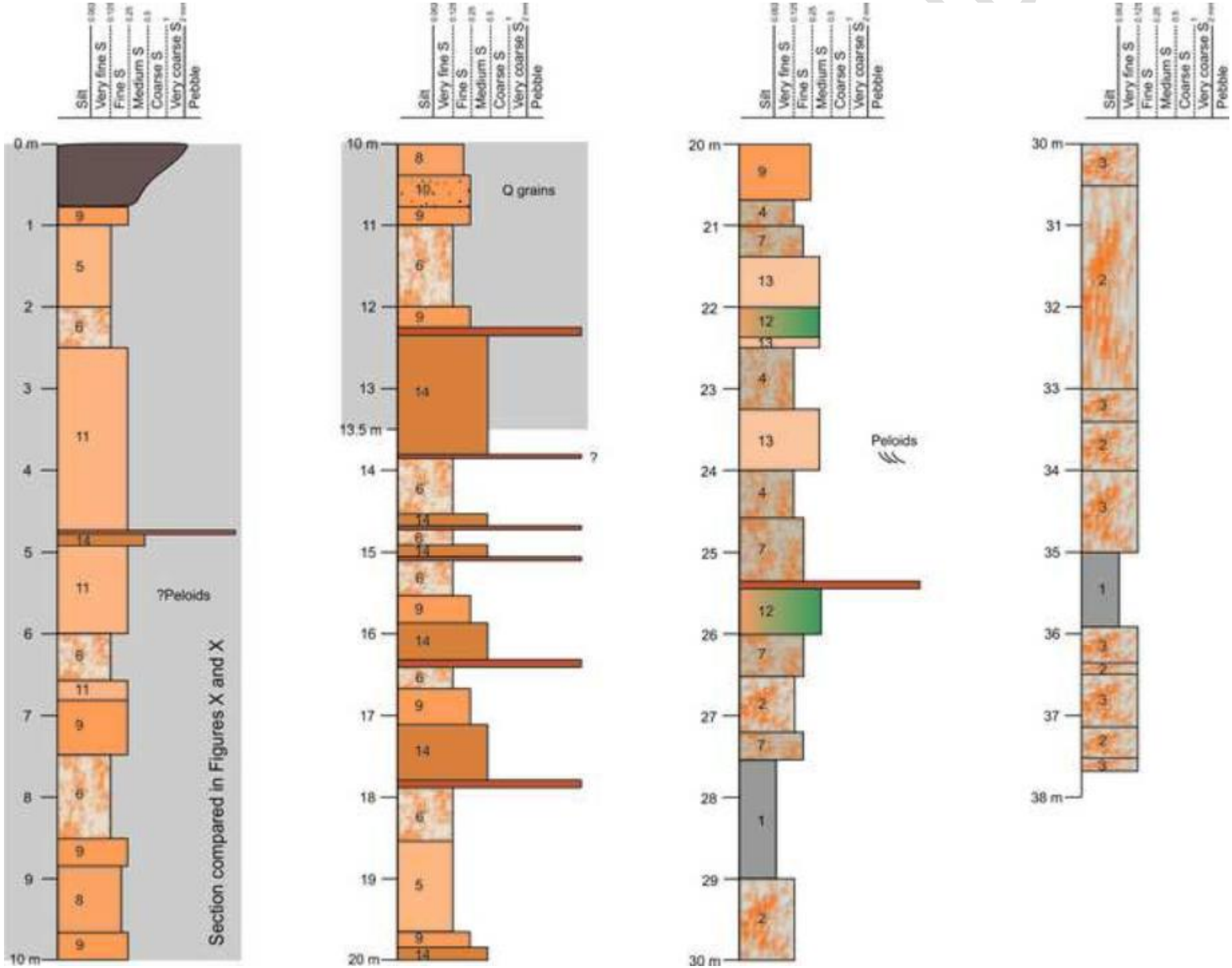

Figure 11
Click here to download high resolution image

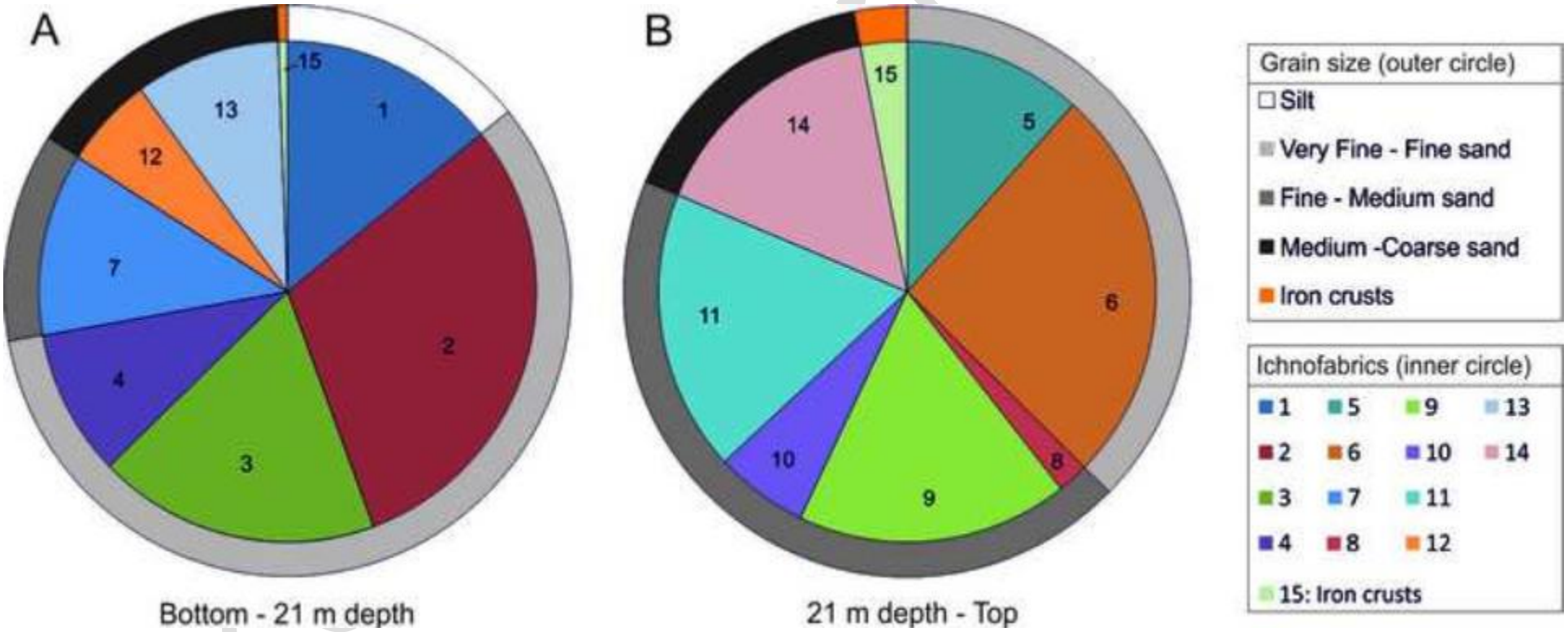

Figure 12

Click here to download high resolution image

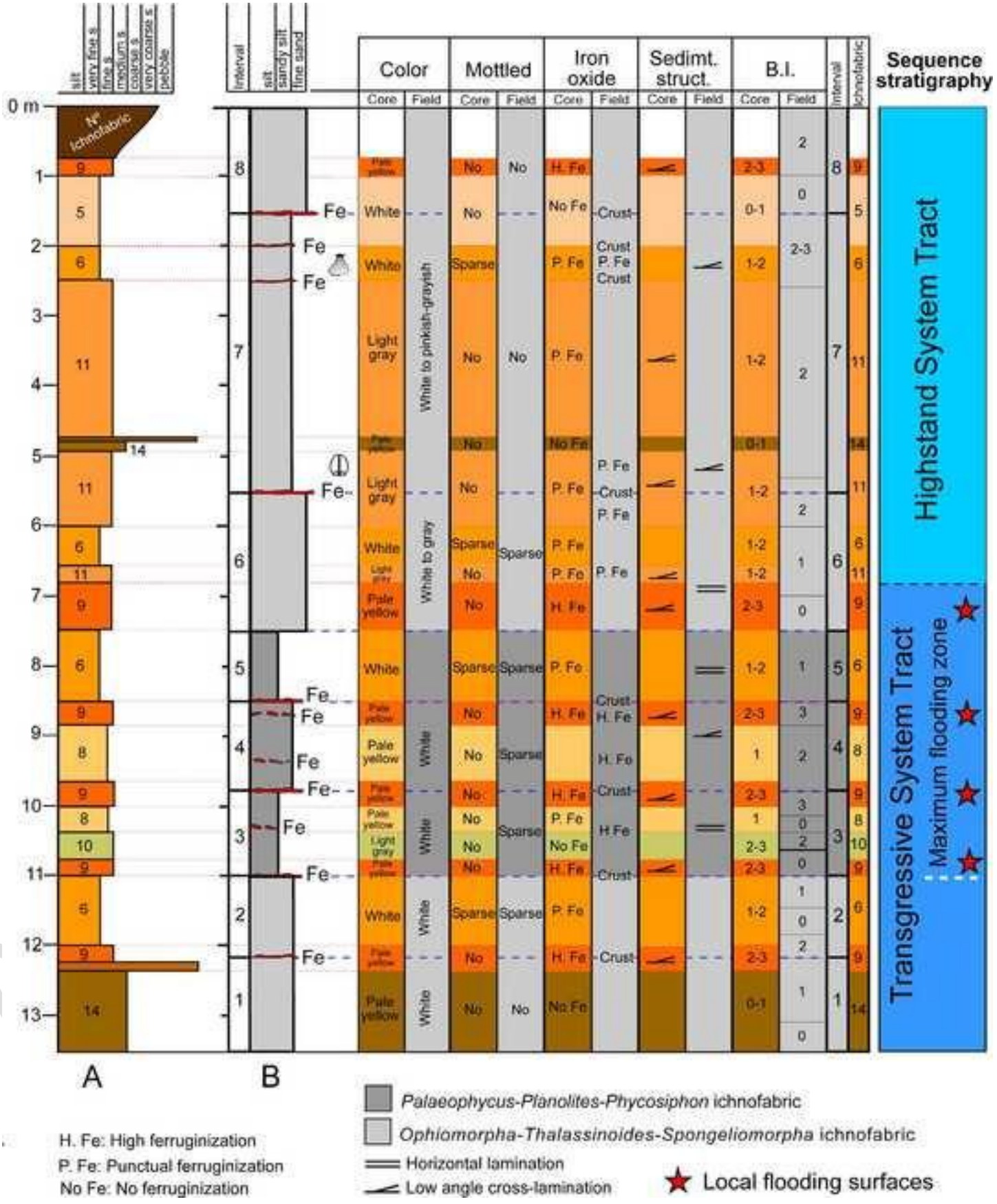

Table 1
Click here to download Table: Table 1.docx

Table 1. Differentiated ichnofabrics in core Lepe S1 (1 to 14) with relevant features.

Ichnofabric	Sediments	Munsell colour	BI	Trace fossils	Mottling	Iron oxide	Sedimentary structures	Other relevant features
1	Silt	Light grey (2.5Y 7/1)	0-1	*Phycosiphon*, *Planolites*, *Thalassinoides* (Fe)				
2	Very fine-fine silty sand	Pale yellow (2.5Y 7/3)	0-1	*Planolites*	Highly mottled	Low		
3	Very fine-fine silty sand	Pale yellow (2.5Y 7/3)	2-3	*Gyrolites*, *Planolites*, *Thalassinoides*	Highly mottled	Abundant	Local cross lamination	Peloids
4	Very fine-fine silty sand	White (2.5Y 8/1)	2-3	*Planolites*, *Thalassinoides*	Scarcely mottled	Locally abundant		
5	Very fine-fine silty sand	White (2.5Y 8/1)	0-1	*Phycodes*				
6	Very fine-fine silty sand	White (2.5Y 8/1)	1-2	*Palaeophycus*, *Planolites*, *Phycosiphon*, *Schaubcylindrichnus*	Scarcely mottled	Low		
7	Fine sand	Pale yellow (2.5Y 8/2)	2-3	*Gyrolites* (Fe), *Planolites*, *Thalassinoides* (Fe)	Highly mottled	Abundant. Infilling traces		
8	Fine sand	Pale yellow (2.5Y 8/3)	1	*Planolites*, *Ophiomorpha* (Fe), *Teichichnus* (Fe)		Low		
9	Fine-medium sand	Pale yellow (2.5Y 8/2)	2-3	*Ophiomorpha* (Fe), *Planolites*, *Schaubcylindrichnus*, *Teichchnus* (Fe)		Abundant	Local cross lamination	
10	Fine-medium sand	Light grey (2.5Y 7/2)	2-3	*Macaronichnus*, *Ophiomorpha*, *Planolites*				Quartz grains
11	Fine-medium sand	Light grey (2.5Y 7/2)	1-2	*Ophiomorpha* (Fe), *Planolites*, *Thalassinoides* (Fe)		Low	Local cross lamination	Peloids
12	Medium sand	White (5Y 8/1)	1-2	*Gyrolites*				
13	Medium sand	White (5Y 8/1)	1-2	*Gyrolites*, *Planolites*, *Thalassinoides*		Low	Local cross lamination	Abundant peloids
14	Medium-coarse sand	Pale yellow (2.5Y 7/3)	0-1	*Conichnus*, *Phycodes*			? Lamination	

Table 2
Click here to download Table: Table 2.docx

Table 2. Transitions (in %) between the differentiated ichnofabrics characterized in correlative 10 cm-thick intervals. Percentage refers to the times that one ichnofabric (column) transits to another one (row), from bottom to top. In italics, the values corresponding to ichnofabrics recognized only in the lower part, and non-italics those recognized in the upper one. Column 15 (values in gray) represents iron crust, identified in both halves.

	1	2	3	4	5	6	7	8	9	10	11	12	13	14	15
1		*16.4*	*17*												
2		*33*					*25*								
3	*50*	*67.2*													
4							*50*						*33.3*		
5						10.9			11.2						
6					50				44.2			66.6		28.6	14.3
7	*50*	*16.4*											*33.3*		
8										50				42.7	14.3
9				*33.3*	50	22.4		100							
10									22.1						14.3
11						10.9			11.2						
12							*25*						*33.3*		
13				*66.6*											
14												33.3	*50*		57.1
						10.9			11.2						
15						44.8							*50*	28.6	